Research on Engineering Structures & Materials
www.jresm.org
MIM Research Group

Review Article

Modern approaches to adhesive debonding from smooth substrates with preservation of surface integrity: A review

Dalya Mohammed Yousif [*,a], Alaa Dahham Younis [b]

Mechanical Engineering Department, College of Engineering, University of Mosul, Mosul, Iraq

Article Info

Article History:

Received 20 July 2026

Accepted 01 Sep 2026

Keywords:

Adhesive debonding;
Smooth substrates;
Surface integrity;
Surface roughness;
Debonding-on-demand;
Post-debonding characterization

Abstract

Adhesive joining has displaced mechanical fastening in a growing share of aerospace, biomedical, electronic and architectural assemblies, mainly because bonded joints spread load more evenly, add little weight and tolerate dissimilar adherends. The reverse operation, separating the adhesive again without marking the part underneath, has attracted far less attention, and it becomes particularly awkward when the substrate is smooth: a polished metal coupon, a float-glass pane, a thinned silicon wafer or an optical-grade polymer presents a uniform, defect-free interface that offers none of the stress concentrators most debonding processes rely on. Removal procedures chosen without regard for the adherend leave micro-scratches, thermally altered layers, chemisorbed residues or dimensional drift, all of which shorten the service life of the recovered component. In this work, we systematically reviewed the literature on mechanical, thermal, chemical, electrochemical and hybrid debonding and assessed each family against the condition of the recovered substrate rather than against removal speed alone. Surface roughness, subsurface hardness, residual stress, chemical state and wettability were adopted as the assessment framework, and the available characterization techniques were compared by the depth of material each actually interrogates. Across the studies surveyed, laser and laser-chemical hybrid routes returned the closest match to the pre-bonding baseline, with roughness increments of roughly 0.05–0.10 μm on metals and composites and below 1 nm in wafer-level release, whereas mechanical scraping produced the largest degradation, up to about 2.3 μm. Chemical routes avoid mechanical damage but leave carbon-rich films that only surface-sensitive spectroscopy detects. We argue that the absence of an agreed post-debonding evaluation protocol, rather than any shortage of removal techniques, is now the main obstacle to progress in the field, and we indicate where responsive adhesives, inline verification and greener chemistries are most likely to develop.

1. Introduction

1.1. From Animal Glue to Load-Bearing Joints

Joining by adhesion is older than metallurgy. Birch-bark tar held stone points to wooden shafts in the Middle Palaeolithic, and animal glues, casein and natural resins carried cabinetmaking, bookbinding and marquetry through to the industrial revolution. What changed in the twentieth century was the chemistry rather than the idea. Phenolic and phenolic-poly(vinyl formal) systems introduced during the 1940s made it possible, for the first time, to pass primary structural load through a bonded metal joint; epoxies followed within the decade and became the reference chemistry for structural bonding, a position they still hold [1]. Bonded doublers, metal-to-metal laminates and honeycomb panels were routine in airframes by the 1970s, and the later expansion

*Corresponding author: dalya.24enp33@student.uomosul.edu.iq
[a]orcid.org/0009-0000-8144-2027; [b]orcid.org/0000-0001-5145-5716
DOI: http://dx.doi.org/10.17515/resm2026-1940st0720rv

of acrylics, polyurethanes, silicones and cyanoacrylates gave designers a chemistry for almost any combination of adherends [1, 2].

1.2. Industrial Importance of Adhesive Bonding

The commercial argument for bonding is straightforward. A bonded overlap transfers load through the whole joint area instead of through a few holes, so peak stresses fall, fatigue performance improves and the fastener holes that act as crack starters disappear [2, 3]. Because no melting is involved, materials that cannot be welded to each other, such as aluminium to carbon-fibre-reinforced polymer (CFRP) or glass to metal, can be joined without distortion [4, 5]. Multi-material light weighting in automotive body structures has become almost entirely dependent on this capability [4], and bonded flush repairs are now an accepted route for restoring damaged composite aerostructure [3, 6].

Bonding is equally embedded in sectors where the joint is never expected to be permanent. Semiconductor manufacturing relies on temporary adhesives to hold device wafers to rigid carriers during thinning and through-silicon-via processing, after which the wafer must be released without cracking or contaminating it [7, 8, 9]. Medical practice attaches dressings, sensors and ostomy appliances to skin that is often fragile [10, 11], and the surgical adhesives now entering clinical use raise the same removal question in a biological setting [12, 13]. Structural silicone carries the dead load of glazed curtain walls [14, 15], and ethylene-vinyl acetate (EVA) encapsulant laminates every crystalline-silicon photovoltaic module in service [16, 17].

1.3. Debonding: The Neglected Half of The Joint Life Cycle

Every one of those applications eventually requires the joint to be opened. The reasons are prosaic and recurrent: rework of misaligned assemblies, warranty repair, failure analysis, replacement of a degraded seal, and, increasingly, recovery of materials at end of life [18, 19, 20]. Regulatory pressure on recyclability has turned what was once a workshop nuisance into a design constraint, and a substantial literature on debondable and debonding-on-demand adhesives has grown up in response [21, 22].

Shop-floor practice, however, has moved much more slowly. Heat guns, chisels, oscillating wire, abrasive discs and solvent soaking remain the standard toolkit. They are cheap and universally available, but they are operator-dependent, essentially uninstrumented, and judged almost exclusively by whether the parts separate [19, 23, 24]. The adherend tends to be treated as a by-product of the operation rather than as the object being recovered. That distinction matters whenever the part is expensive, is to be rebonded, or has to meet an optical, sealing or fatigue specification after reassembly [25, 26].

1.4. Why Surface Integrity is the Correct Measure of Success

Surface integrity, in the sense established for machined components, is not a single number. It bundles together the topography of the outermost surface, the microstructure and hardness of the layer immediately beneath it, the residual stress state, and the chemical composition of the first few nanometers [27]. Each of these has an established engineering consequence, which is why we adopt it here as the axis along which debonding methods are compared.

Roughness is the most frequently reported parameter and the most frequently misused. An increase in Ra after debonding is not merely cosmetic: roughness peaks act as stress concentrators and shorten fatigue life, an effect quantified repeatedly for machined and additively manufactured metals [28, 29]. Roughness also changes the effective bonding area, so a substrate that has been scraped will not rebond with the same interfacial behaviour as the original [30, 31].

Microhardness and the associated subsurface deformation field record whether the removal process worked the material rather than merely the adhesive. Hardness depth profiles are the conventional way of revealing a work-hardened or thermally softened layer, and they respond to processing history well below the depth that a profilometer can see [27].

Residual stress is the parameter most often ignored in debonding studies and arguably the most consequential. Tensile residual stress introduced at the surface accelerates fatigue crack initiation

and stress-corrosion cracking, whereas a compressive state is protective; the relationship between surface roughness, residual stress and fatigue life has been established quantitatively for several alloy systems [28, 27, 29].

Corrosion resistance depends on the continuity of the passive oxide film. Any operation that abrades, thermally alters or chemically strips that film exposes fresh metal, and on aluminium and stainless steel the recovered joint can become the corrosion-critical location of the assembly [32, 33]. Optical performance is even less forgiving: in interferometric and photonic assemblies, surface figure changes of a few nanometers are already out of specification [34, 35]. In biomedical use the requirement shifts from topography to chemistry, since residual solvent or adhesive on a surface that will contact tissue is a contamination issue before it is a mechanical one [12, 13, 10].

1.5. Why Smooth Substrates Require Separate Treatment

We restrict this review to substrates whose as-received arithmetic mean roughness Ra is below approximately 0.8 μm, the value conventionally associated with a fine-machined, ground or polished finish. The limit is a working convention rather than a physical constant, but it separates two genuinely different adhesion regimes.

On a deliberately roughened substrate, a significant part of the bond strength comes from mechanical interlocking: adhesive penetrates the relief left by grit blasting or laser texturing and is held by geometry as much as by chemistry. Laser-texturing studies show this directly, with lap-shear strength rising steeply as the processed roughness is increased over a controlled range [30, 31, 5]. Below roughly 0.8 μm the asperity relief becomes small compared with the adhesive layer thickness, real contact area approaches the nominal area, and adhesion is carried instead by wetting, adsorption and chemical interaction across an interface that is close to planar.

Three consequences follow, and together they justify treating smooth substrates as a distinct problem. First, the interfacial stress distribution is nearly uniform, so there is no natural crack starter; separation must be initiated artificially, which is precisely why smooth joints resist gentle methods and invite aggressive ones. Second, the tolerance for damage is far lower. A 2 μm scratch is invisible within the profile of a grit-blasted surface but is the dominant feature on a polished mirror, a float-glass pane or a thinned wafer. Third, damage on a smooth substrate is usually irreversible in practice, because restoring an optical or sealing finish means re-polishing, which removes material and alters dimensions. For these reasons the surface integrity criterion becomes binding on smooth substrates in a way it simply is not on rough ones.

1.6. Relation to Previous Reviews and Contribution of the Present Work

Debonding has been reviewed before, but from other vantage points. Srinivasan and Idapalapati surveyed debonding of adhesively bonded composite structures with sustainability as the organizing theme and with composites as the only substrate class [19]. Mulcahy and co-workers reviewed debondable adhesive chemistries in the context of recycling, treating the adhesive rather than the adherend as the object of study [18]. Blelloch et al. and Liu and Yan covered stimuli-responsive and switchable adhesion from a molecular-design perspective [21, 22]. Mo et al. reviewed temporary bonding and debonding specifically within advanced semiconductor packaging [7], and Ghahremani et al. confined their analysis to delamination of waste photovoltaic panels [23]. Laser cleaning has its own review literature, but it addresses coatings and contamination generally rather than adhesive joints [36, 32].

None of these takes the recovered substrate surface as the primary evaluation axis, and none cuts across substrate classes. The present review is intended to fill that gap, and it differs from its predecessors in five specific ways. It is substrate-centered rather than adhesive-centered and organizes evidence by what happens to the adherend. It covers five substrate families and five method families within a single comparative frame, so that a decision can be made for a given material rather than for a given chemistry. It arranges the characterization toolbox by information depth, which is the only way that roughness data, spectroscopic data and hardness data from different studies can be read together. It consolidates the scattered quantitative roughness

evidence into a single comparison. Finally, it is explicitly bounded to smooth substrates, where the surface integrity constraint is at its most severe.

The remainder of the paper is organized as follows. Section 2 classifies smooth substrates and their sensitivities. Section 3 summarizes adhesive chemistries and the debonding triggers each expose. Section 4 reviews the debonding methods themselves. Section 5 deals with characterization, Section 6 with comparative performance, Section 7 with industrial application, and Section 8 with the open problems we consider most limiting.

2. Classification of Smooth Substrates

For the purposes of this review, a smooth substrate is any solid surface presenting an as-received Ra below approximately 0.8 µm together with good dimensional consistency and a reasonably well-defined surface energy. Classification matters in debonding work because composition, surface free energy, thermal conductivity and chemical reactivity between them decide which removal mechanisms are admissible and what the recovered surface will look like. The six classes below are ordered by how commonly they appear in the debonding literature. Their properties are compared in Table 1 and their relationships summarized in Figure 1.

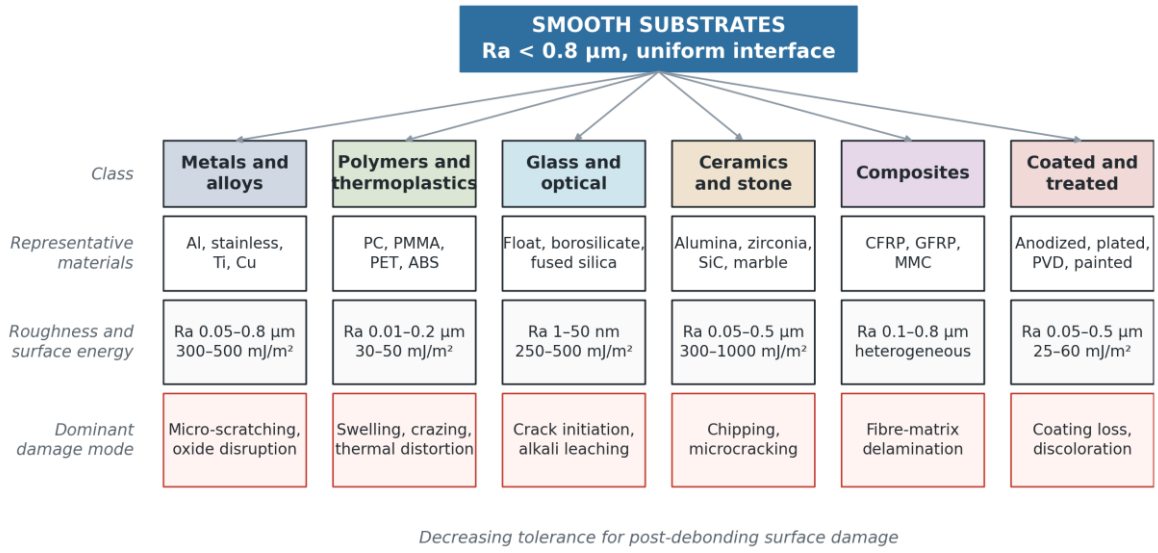

Fig. 1. Classification of smooth substrates used in this review, with the indicative as-received roughness range, surface free energy and dominant damage mode of each class

2.1 Metals and Alloys

Aluminium alloys, stainless steels, titanium alloys and copper form the most extensively studied group. Surface free energies in the range of roughly 300–500 mJ/m^2 on a cleaned, oxide-covered surface promote excellent wetting and strong adhesion, which is exactly what makes damage-free separation difficult [30, 31]. The characteristic surface integrity concerns are micro-scratching and plastic smearing from contact tools, disruption of the passive oxide, embedded abrasive or tool material, and retained organic contamination [37, 38]. Because metals conduct heat well, thermal methods spread energy away from the bondline efficiently, which is helpful for the substrate but often means the adhesive itself never reaches its softening temperature.

2.2 Polymers and Thermoplastics

Polycarbonate, poly(methyl methacrylate), poly(ethylene terephthalate), poly(vinyl chloride) and acrylonitrile-butadiene-styrene are used in electronic enclosures, optical components and medical device housings, usually with a molded or extruded finish that is already smooth. Their low surface free energy, typically 30–50 mJ/m^2, limits interfacial adhesion and makes controlled separation easier in principle [4]. In practice they are the most vulnerable class, because the same softening temperature and solvent sensitivity that make debonding possible also damage the substrate:

thermal distortion begins not far above the glass transition, polar solvents induce swelling, crazing and stress cracking, and the low hardness means any contact tool leaves a mark [16, 39].

2.3. Glass and Optical Substrates

Soda-lime float glass, borosilicate and fused silica are used in architectural glazing, display assemblies and photovoltaic front sheets. Fusion-drawn and float surfaces are among the smoothest engineering surfaces available, with Ra of the order of a nanometer and in all cases well below 0.05 μm, and a freshly cleaned, hydroxyl-terminated surface presents a high surface energy that silanol-coupled adhesives exploit efficiently [40, 15]. Two properties govern their debonding behaviour. Glass is brittle and has no plastic reserve, so any tensile or bending stress imposed during separation propagates from pre-existing surface flaws and initiates cracking rather than yielding [41]. Glass is also chemically alterable: strongly alkaline media leach network-modifying alkali ions and permanently change the surface composition, so chemical assistance has to be selected with the substrate and not only the adhesive in mind [42].

2.4. Ceramics and Stone

Alumina, zirconia and silicon carbide are used in cutting tools, dental prostheses and wear components, while marble and granite appear as architectural cladding bonded with structural adhesive. These materials combine very high hardness with low fracture toughness, and the combination is unhelpful: they resist abrasive damage better than metals do, but they respond to a locally applied mechanical load by chipping or by initiating a microcrack rather than by deforming [43]. Chemical methods must be screened against the specific composition, since acidic media attack glassy grain-boundary phases in sintered ceramics and carbonate-based stone dissolves outright.

2.5. Composite Materials

Carbon- and glass-fibre-reinforced polymers and metal-matrix composites dominate aerospace and high-performance automotive structures, and their tool-side surfaces are frequently smooth enough to fall within the scope of this review [3, 44]. Three features complicate their debonding. The surface energy is heterogeneous at the scale of the fibre spacing, so adhesion is not uniform. The mechanical response is anisotropic, and a load that is safe in the fibre direction may not be safe transverse to it. Most importantly, the resin-rich surface layer is thin, and removing it exposes fibre and initiates fibre-matrix delamination, a form of damage that is not detectable by roughness measurement and not repairable [19, 45].

2.6. Coated and Surface-Treated Substrates

Anodized aluminium, electroplated components, physical-vapor-deposited coatings and painted panels behave as composite surfaces in which the functional layer may be only a few micrometers thick. Debonding behaviour is set by the coating rather than by the bulk material, and the failure mode of concern is loss of the coating itself through delamination, discoloration or dissolution [46, 24]. Automotive glazing removal is the canonical example: the polyurethane bead must be cut away while the electrocoat and topcoat on the flange survive intact [4].

3. Adhesive Systems and Their Bonding Mechanisms

Choosing a debonding route without knowing the adhesive chemistry is guesswork. Composition, cure mechanism and thermal behaviour together decide what kind of interfacial bond exists and which stimulus can be used to break it, and they also decide what will be left behind [2, 1]. The classes below are summarized in Table 2.

3.1. Epoxy Adhesives

Epoxies remain the reference structural chemistry. The most common formulations are based on the diglyceryl ether of bisphenol A (DGEBA), cured irreversibly with amine or anhydride hardeners through opening of the terminal oxirane rings, which builds a three-dimensional covalent network whose crosslink density is set by the hardener and the cure schedule [47, 48]. Adhesion to a smooth metal arises from a combination of van der Waals interaction, hydrogen bonding to surface

hydroxyls and, on primed surfaces, covalent bonding; reported lap-shear strengths on prepared metallic substrates typically fall between about 15 and 45 MPa [1, 2]. The same network structure that gives epoxies their strength also explains their debonding behaviour: because the network is covalently continuous, a cured epoxy cannot dissolve, it can only swell, and thermal or chemical scission of the network is required before it will release. The DGEBA structure and its amine cure are shown in Figure 2.

Table 1. Comparison of smooth substrate classes relevant to adhesive debonding

Substrate class	Representative materials	As-received Ra	Surface free energy (mJ/m^2)	Typical applications	Dominant debonding risk	Damage susceptibility
Metals and alloys	Al alloys, stainless steel, Ti, Cu	0.05–0.8 µm	300–500	Airframe skins, housings, heat sinks	Micro-scratching, oxide disruption, embedded contamination	Moderate to high
Polymers and thermoplastics	PC, PMMA, PET, PVC, ABS	0.01–0.2 µm	30–50	Enclosures, optical parts, device housings	Solvent swelling and crazing, thermal distortion, abrasion	High
Glass and optical	Soda-lime float, borosilicate, fused silica	1–50 nm	250–500 (freshly cleaned)	Glazing, displays, PV front sheets	Crack initiation from surface flaws, alkali leaching, staining	Very high
Ceramics and stone	Alumina, zirconia, SiC, marble, granite	0.05–0.5 µm	300–1000	Cutting tools, dental prostheses, cladding	Chipping, microcracking, grain-boundary attack	High
Composites	CFRP, GFRP, metal-matrix composites	0.1–0.8 µm	Heterogeneous, 35–60 for matrix	Aerostructure, automotive body panels	Fibre-matrix delamination, loss of resin-rich layer	Very high
Coated and treated	Anodized Al, electroplate, PVD, paint	0.05–0.5 µm	25–60 (coating dependent)	Body flanges, decorative and functional coatings	Coating delamination, discoloration, dissolution	High

Values are indicative ranges compiled from the sources cited in Section 2 and are intended for comparison between classes, not as specification data.

3.2. Acrylic and Methacrylate Adhesives

Two distinct families share this heading. Pressure-sensitive adhesives develop adhesion by viscoelastic flow into contact under light pressure, holding through van der Waals interaction and hydrogen bonding without any chemical reaction; their bond strength is rate- and temperature-dependent and is normally reported as a peel force per unit width rather than as a shear stress [49]. Reactive acrylic and methacrylate systems polymerize by a free-radical mechanism to give tough networks of lower crosslink density than epoxies. That lower density is significant for debonding, because it leaves the network accessible to solvent penetration and, in lightly crosslinked grades, to genuine dissolution [2].

3.3. Polyurethane Adhesives

Polyurethanes are chosen where flexibility, impact resistance and accommodation of differential thermal expansion matter, which is why they dominate windscreen bonding and construction sealing [4]. Bonding proceeds through reaction of isocyanate groups with polyols and with adsorbed surface moisture, giving urethane and urea linkages and, on hydroxylated substrates, true covalent interfacial bonds. Thermoplastic grades soften on heating, and this reversibility is the basis of the heated-wire cutting used in automotive glass replacement [50].

3.4. Silicone adhesives and sealants

Structural silicones are built on a polydimethylsiloxane backbone and cure by condensation or by addition at ambient temperature. The Si-O-Si chain is unusually flexible and the glass transition lies

near −120 °C, which is why these materials remain elastomeric over the whole service range of a building facade and why elongation at break well above 100% is normal for structural glazing grades [14, 40]. Adhesion is predominantly physical, through dispersive interaction, and is supplemented by covalent coupling where organ silane primers have been used. Silicones are the most difficult class to remove completely: their very low surface energy means that the last molecular layers wet the substrate strongly and are not displaced by solvents, so a low-energy siloxane residue typically survives cleaning and prevents subsequent rebonding [14, 51].

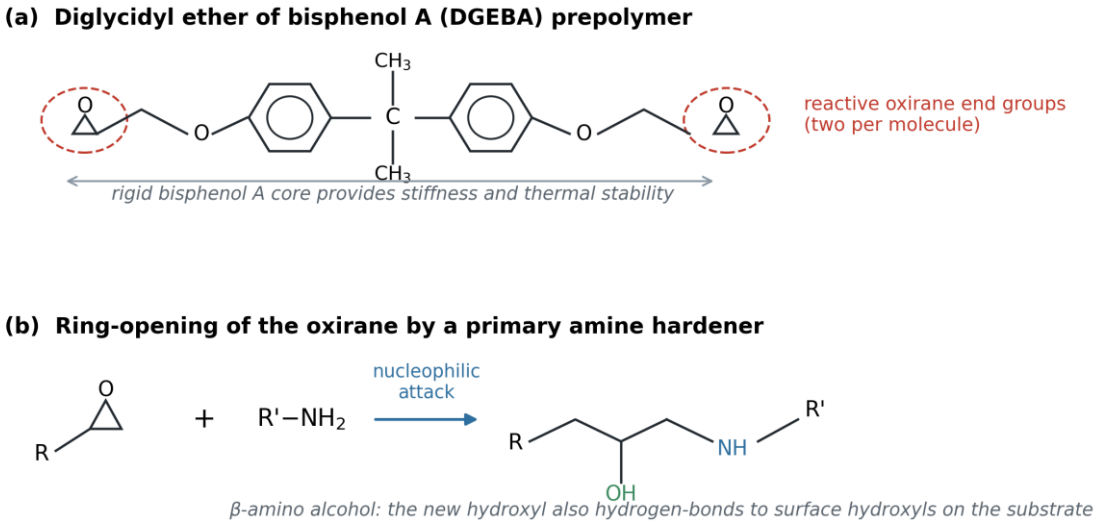

Fig. 2. Chemistry of DGEBA-based epoxy adhesives: (a) the DGEBA prepolymer; (b) ring-opening of the terminal oxirane by a primary amine; (c) build-up of the crosslinked network, whose covalent continuity prevents dissolution and restricts solvent action to swelling

3.5. Cyanoacrylate Adhesives

Cyanoacrylates polymerize anionic ally within seconds, initiated by the water film that is present on any surface exposed to ambient humidity, and form a rigid, essentially linear poly(alkyl cyanoacrylate). Because the polymer is linear rather than crosslinked, it is susceptible to polar aprotic solvents, and acetone, dimethyl sulfoxide and nitromethane dissolve rather than merely swell it. This is the one adhesive class for which true solvent dissolution, as opposed to swelling, is a practical debonding route [2].

3.6. Hot-Melt Adhesives

Hot melts are thermoplastics applied as a melt that develop adhesion purely on solidification, with no chemical reaction involved. Their reversibility is complete in principle: heating above the softening point restores the melt and the joint opens with minimal force [9]. They are consequently the easiest class to debond and the least demanding on the substrate, provided the substrate itself tolerates the temperature.

3.7. Bonding Mechanisms at A Smooth Interface

Five mechanisms are generally recognized, and their relative weight shifts markedly when the substrate is smooth. Mechanical interlocking, which dominates on textured surfaces, is reduced to whatever nanoscale relief remains and contributes comparatively little [30, 31]. Adsorption and wetting, governed by the thermodynamic work of adhesion, become correspondingly more important, as does chemical bonding through primers and coupling agents, which produces the strongest and most durable interfaces [37]. Electrostatic interaction and interdiffusion play a part at polymer-polymer interfaces but are minor at polymer-metal and polymer-glass interfaces [4]. The practical implication for this review is that on smooth substrates the bond is carried by short-range interactions distributed uniformly across the contact area, which is precisely the configuration that resists crack initiation. Figure 3 summarizes these mechanisms.

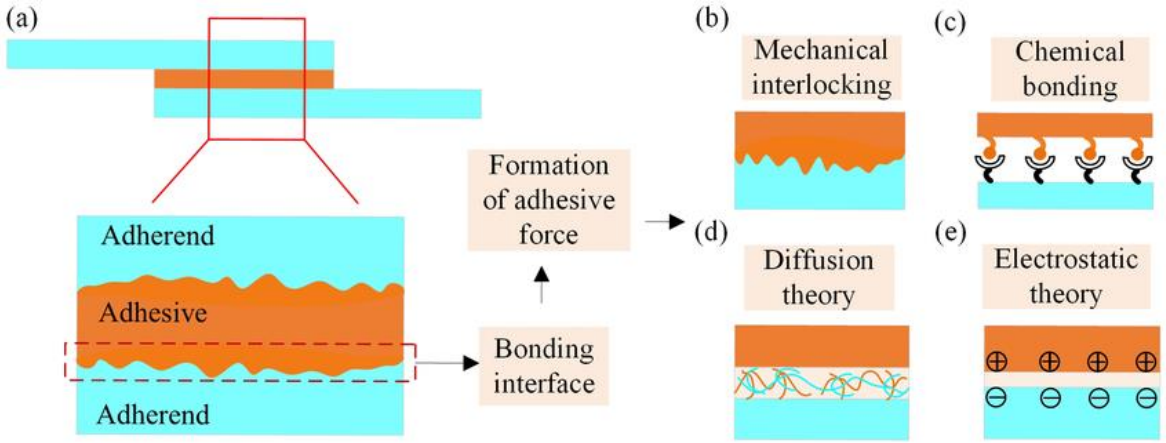

Fig. 3. Bonding mechanisms operating at an adhesive-substrate interface

The corresponding question, and the one that organizes Section 4, is what physical process can be introduced to defeat each mechanism. Figure 4 sets out the three stimuli that recur throughout the debonding literature: thermal relaxation of the polymer network above its glass transition, penetration and swelling of the network by a matched solvent, and electrochemical generation of gas at the interface itself.

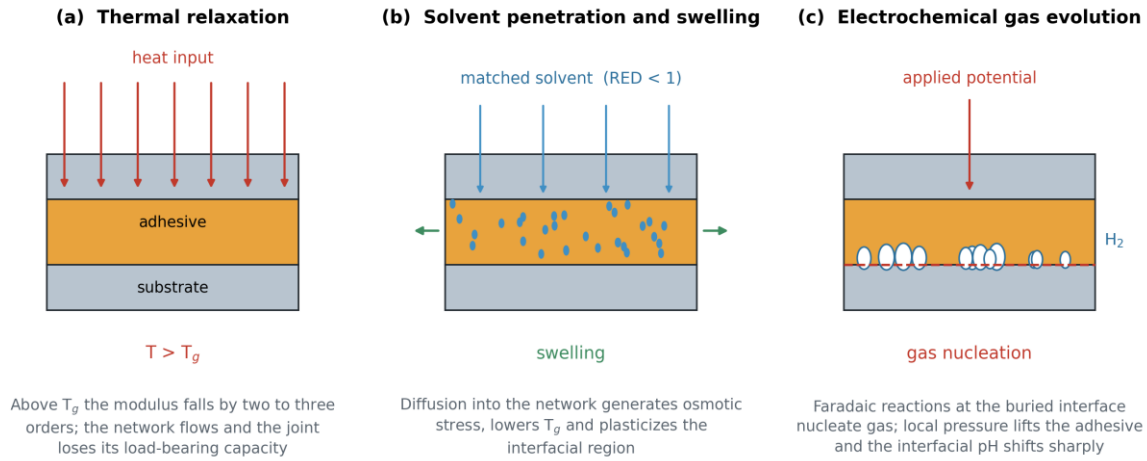

Fig. 4. Principal debonding stimuli at a smooth interface: (a) thermal relaxation, in which heating above the glass transition collapses the modulus and the load-bearing capacity of the network; (b) solvent penetration and swelling, in which diffusion into the network generates internal osmotic stress and plasticizes the interfacial region; (c) electrochemical gas evolution, in which faradaic reactions at the buried interface nucleate hydrogen or oxygen bubbles that lift the adhesive locally

Table 2. Adhesive classes, bonding mechanisms and the debonding triggers each expose

Adhesive class	Bonding and cure mechanism	Indicative strength on smooth substrate	Practical debonding trigger	Residual surface effect
Epoxy (DGEBA-amine)	Irreversible thermoset network; van der Waals, hydrogen and covalent bonding	15–45 MPa lap shear	Heating above T_g, laser ablation, strong alkali or acid; solvents swell only	Thin crosslinked residue; carbon-rich film detectable by XPS
Reactive acrylic / methacrylate	Free-radical chain growth; moderate crosslink density	10–30 MPa lap shear	Polar solvents, moderate heat, ultrasonic assistance	Partly dissolved and swollen residue
Pressure-sensitive acrylic	Viscoelastic contact; van der Waals and hydrogen bonding	0.2–1.5 N/mm peel	Peel angle control, cooling below T_g, solvent	Tackifier and plasticizer transfer film
Polyurethane	Isocyanate-polyol and isocyanate-water reaction; urethane and urea linkages	8–25 MPa lap shear	Thermal softening of thermoplastic grades, heated-wire cutting, alkaline hydrolysis	Soft residue; possible staining of coated substrates
Silicone (RTV and structural)	Condensation or addition cure of PDMS; dispersive interaction plus silane coupling	0.7–2 MPa tensile (structural glazing)	Mechanical cutting with chemical softening; thermally activated debonding-on-demand grades	Low-energy siloxane residue; the hardest class to remove completely
Cyanoacrylate	Anionic polymerization initiated by adsorbed water; linear polymer	15–25 MPa lap shear	Acetone, DMSO, nitromethane; heating above about 150 °C	Brittle flakes; genuine dissolution possible
Hot melt	Physical solidification of a thermoplastic melt; no reaction	1–8 MPa lap shear	Heating above the softening point	Thermoplastic film, readily wiped away

Strength figures are indicative values reported for well-prepared smooth substrates and vary strongly with surface preparation, bondline thickness and test geometry.

4. Debonding Methods

The methods described below differ in operating principle, in the process parameters that control them, in the range of substrates they suit, and above all in what they leave behind. Figure 5 places them in a common framework. We have kept the conventional division into mechanical, thermal, chemical, electrochemical and hybrid families, with one change relative to earlier treatments: cryogenic debonding is discussed under thermal methods, since it operates through the same mechanism of imposed temperature change and differential thermal strain, merely in the opposite direction.

4.1. Mechanical Debonding

4.1.1. Controlled Peeling

Peeling applies a tensile force at a defined angle to the interface and concentrates the resulting stress into a narrow peel front, which then advances along the bondline. The peel angle is the controlling variable. At angles approaching 90 degrees the loading at the front is predominantly

tensile, separation is progressive and substrate deformation is small; at low angles a substantial shear component is superimposed, and on soft or coated substrates this produces micro-tearing and smearing rather than clean separation [49]. Reported peel forces fall steeply as the peel angle is increased from a few degrees towards 90 degrees, after which the dependence weakens considerably, so operating near or above 90 degrees is advantageous both for the force required and for the damage produced [49]. Peeling is only available where at least one adherend is flexible enough to be bent to the peel radius, which excludes glass, ceramics and most thick metallic sections.

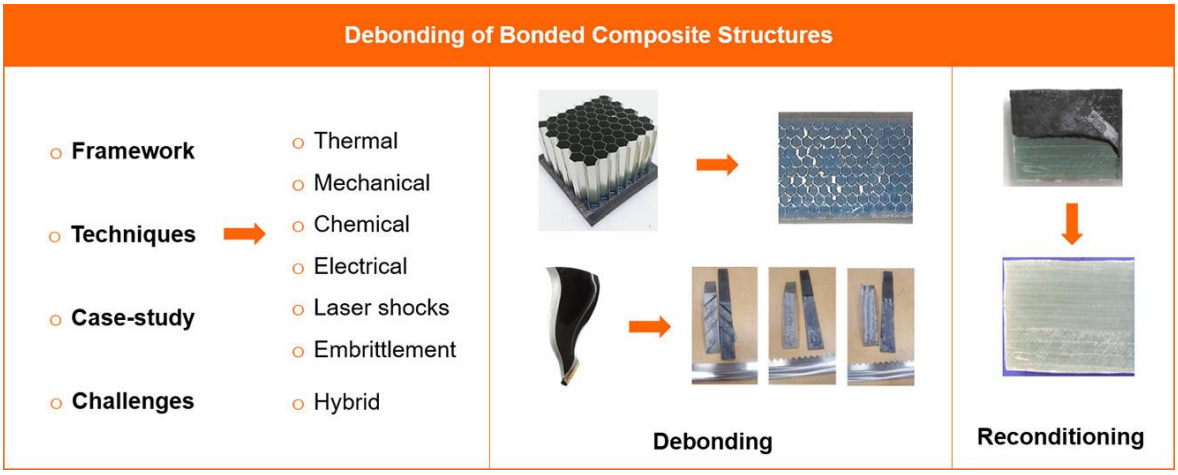

Fig. 5. Debonding techniques in adhesive joints. Adapted from [19]

4.1.2. Scraping and Abrasion

Scraping is the default workshop method and the worst performer in surface integrity terms. Material is removed by combined shear and compression under a hand-held or powered tool, and the damage produced scales with the hardness differential between tool and substrate, the applied normal load, the sliding velocity and the edge geometry of the tool. Where quantified, the differences between tools are large. In dental work, which is one of the few fields in which post-removal roughness is measured routinely, the four common protocols for removing residual orthodontic adhesive from enamel produced significantly different final roughness, with rotary carbide instruments leaving the roughest surfaces and finishing sequences recovering only part of the original condition [52, 43]. The same ordering, if not the same absolute values, holds for engineering substrates: across the studies surveyed here, mechanical scraping raised Ra by roughly 0.3–2.3 μm, an order of magnitude more than any non-contact method [19, 23]. Substituting polymer or wooden tools for steel reduces but does not eliminate the effect, because the abrasive is often the detached adhesive itself, which carries entrained hard particles.

4.1.3. Ultrasonic Vibration Debonding

Ultrasonic methods, generally operated between 20 and 40 kHz, are the most effective mechanical route on smooth substrates and deserve more attention than they have received. Four mechanisms act together, and separating them is important because they respond to different process parameters [53].

The first is acoustic cavitation, which occurs when the process is carried out in a liquid. The negative pressure half-cycle nucleates vapor cavities that collapse asymmetrically near the solid boundary, producing microjets and local shock loading directed at the interface. Cavitation is what makes ultrasonic cleaning effective at removing adherent films, and in a debonding context it delivers energy to the bondline without any tool touching the substrate [39]. The second is cyclic shear: the acoustic field imposes an alternating shear strain across the adhesive layer, and because polymer adhesives are viscoelastic, repeated cycling accumulates damage at stress amplitudes well below the static strength, so the joint fails by a fatigue mechanism rather than by overload [53, 54]. The third is localized heating: the loss modulus of the adhesive converts part of the vibrational energy to heat directly within the bondline, and because the adhesive is a far poorer conductor than

the metal or glass adherend, the temperature rise is concentrated exactly where it is needed while the substrate stays close to ambient [53, 55]. The fourth is resonance. When the excitation frequency is matched to a thickness or layer resonance of the assembly, the displacement amplitude at the interface is amplified substantially for the same input power, and layer-resonance-assisted approaches have been demonstrated for metal plate assemblies [56].

Reported process times range from seconds to a few minutes depending on adhesive class, bonded area and delivered power, and roughness increments as low as about 0.2 μm have been reported on smooth metallic and composite substrates, since no tool contacts the surface [53]. The practical limitations are that brittle substrates can be cracked by resonant amplitudes, and that the acoustic field is difficult to keep uniform over large bonded areas.

4.1.4. Pneumatic and Hydraulic Pressure Methods

Fluid pressure introduced through micro-injection nozzles distributes the separating load over the whole bonded area instead of concentrating it at a tool tip. The approach is useful in large-area assemblies where peeling is impractical, and it minimizes solid contact with the substrate, but it requires an accessible edge or an injection port and generally leaves the adhesive itself in place, so a cleaning step is still needed [6].

4.2. Thermal Debonding

4.2.1. Convective and Conductive Heating

Convective hot air systems and infrared sources operating between about 150 and 350 °C are standard for thermoplastic and hot-melt adhesives. The method is inexpensive and needs no special adhesive formulation, but heat is delivered to the outside of the assembly and has to conduct inwards to the bondline, so the substrate necessarily sees a higher temperature than the adhesive does. On polymers this is the dominant risk, and without good thermal control distortion and discoloration occur before the adhesive softens [9, 4].

4.2.2. Laser Debonding

Laser debonding is the most precise route available and, on the evidence assembled in Section 6, the best performer in surface integrity terms. Its advantage comes from selective absorption: energy is deposited where the optical properties of the material place it, not where the heat happens to conduct. Three wavelength regimes are used and they operate by genuinely different physics, a distinction that is often blurred in the applied literature. The process is illustrated in Figure 6.

Ultraviolet excimer sources, typically KrF at 248 nm or ArF at 193 nm, deliver photons whose energy exceeds the dissociation energy of the carbon-carbon and carbon-oxygen bonds in the polymer backbone. Ablation is therefore largely photochemical: bonds are broken directly and the fragments are ejected before the absorbed energy has time to diffuse as heat, which leaves a very shallow heat-affected zone. This is the basis of laser release through transparent glass carriers in wafer-level packaging, where the absorbing layer is engineered to be a few hundred nanometers thick and the silicon behind it is essentially untouched [7, 57, 42]. Near-infrared Nd:YAG sources at 1064 nm, by contrast, act photothermally: absorption raises the temperature of the adhesive and of any filler within it, and separation follows from thermal expansion, decomposition and the resulting stress wave [58, 59]. Carbon dioxide lasers at 10.6 μm are strongly absorbed by most organic polymers and by glass, which makes them efficient at removing thick organic layers but unsuitable where a glass substrate must survive, since the substrate absorbs as readily as the adhesive.

The surface integrity consequences follow directly from this division. Ultraviolet processing gives the smallest thermal alteration but photochemically oxidizes the exposed surface, which shows up as a marked increase in hydrophilicity rather than as a change in topography. Photothermal processing leaves the topography almost unchanged provided the fluence stays below the substrate ablation threshold, but it can generate a thin recast or oxidized layer. Systematic laser cleaning studies on aluminium alloy show exactly this threshold behaviour, with the substrate

essentially unaffected below a critical fluence and roughness rising once it is exceeded [36, 60, 32]. Post-debonding roughness comparable to the pre-bonding baseline has been demonstrated for composite, glass and semiconductor wafer applications, and in wafer release the recovered surface is held below 1 nm Ra [57, 58].

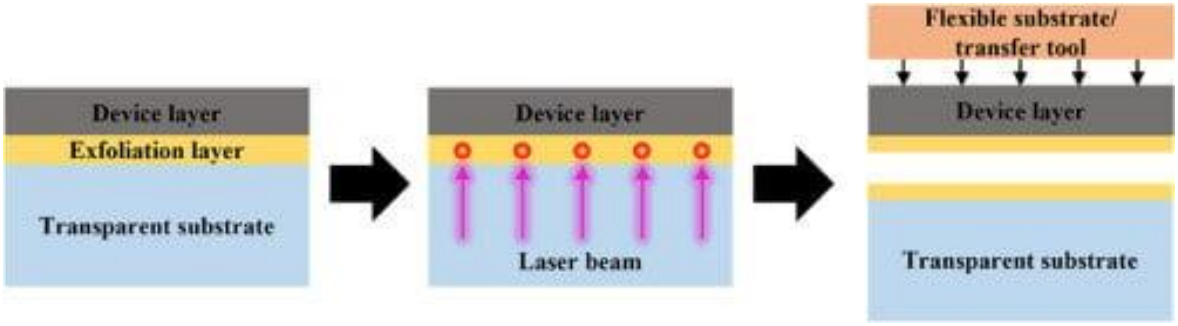

Fig. 6. Schematic of the laser debonding process through a transparent carrier

4.2.3. Induction Heating and Susceptor Fillers

Induction heating generates heat inside the joint rather than outside it, either by eddy currents in a conductive adherend or by hysteresis and relaxation losses in ferromagnetic or superparamagnetic particles dispersed in the adhesive itself. Debonding within 60 seconds has been reported on aluminium alloy substrates with negligible roughness increase, and magnetically responsive nanocomposite interlayers have been demonstrated as a designed debonding-on-demand route for laminated composites [46, 61]. Related concepts use resistive heating of an embedded conductive reinforcement to the same end [62], or expandable graphite fillers that generate separating stress as they intercalate [63].

The reviewer-relevant question is what these fillers cost in joint performance and in surface cleanliness, and the literature is candid about it. Filler loading generally reduces lap-shear strength relative to the unmodified adhesive, because the particles interrupt the continuity of the polymer network and introduce stress concentrations; the loading therefore has to be optimized against the heating rate required [46, 61]. After debonding, the particles do not evaporate. They remain in the residue, and iron oxide or graphite particles adhering to a recovered metal surface constitute both a contamination problem and, in the case of iron on aluminium, a galvanic corrosion risk. Complete removal requires a cleaning step whose own aggressiveness must then be assessed, which is why we regard filler-based routes as well suited to designed disassembly and poorly suited to recovery of optical or electronic surfaces [63].

4.2.4. Cryogenic Debonding

Cooling the assembly with liquid nitrogen or solid carbon dioxide exploits the same physics in reverse. Polymer adhesives have thermal expansion coefficients roughly one order of magnitude larger than metals and two orders larger than glass or silicon, so cooling generates a differential contraction strain that appears as interfacial shear. At the same time the adhesive passes below its glass transition and becomes brittle, so the joint loses the capacity to accommodate that strain by flow. Joints have been reported to separate spontaneously or under very low manual force, without reagents, heat or tool contact [50]. The approach is attractive for temperature-sensitive assemblies and for clean-room use, and the behaviour of adhesives at cryogenic temperature is well documented in the photonic packaging literature [35, 34, 64]. Its limits are equally clear: assemblies with a large thermal expansion mismatch between the adherends themselves may be damaged by the cooling, brittle substrates can crack under thermal shock if the cooling rate is not controlled, and condensation on rewarming introduces a moisture problem of its own.

4.3. Chemical Debonding

4.3.1. Solvent Action: Swelling is not Dissolution

The most common conceptual error in the applied literature is to treat solvent debonding as dissolution. It is worth stating the distinction plainly, because it determines what a solvent can and

cannot achieve. A crosslinked thermoset is a single covalently connected molecule spanning the whole bondline. No solvent can dissolve it, because dissolution requires individual chains to be separated and carried away, and here there are no individual chains. What a well-matched solvent does instead is diffuse into the network and swell it. Swelling generates internal stress, plasticizes the polymer, drops the glass transition temperature and reduces the modulus, and it is this softening, together with the osmotic stress developed at the interface, that opens the joint [65, 39]. Cured epoxies, cured polyurethanes and silicones fall in this category and swell only. Linear or lightly crosslinked polymers, notably poly(alkyl cyanoacrylate), many pressure-sensitive acrylics and hot melts, genuinely dissolve. The practical consequence is that a solvent process designed for a cyanoacrylate joint will disappoint on an epoxy joint no matter how long the immersion, and that solvent treatment of a thermoset should be understood as a softening pretreatment rather than as a removal step in its own right.

Which solvent to choose is not a matter of trial and error. Hansen solubility parameter (HSP) theory splits the cohesive energy density of a liquid into three components: a dispersion term δD from London forces, a polar term δP from permanent dipole interaction, and a hydrogen bonding term δH [66]. Each solvent and each polymer occupy a point in this three-dimensional space, and interaction is predicted by the distance between them,

$$Ra^2 = 4(\delta D1 - \delta D2)^2 + (\delta P1 - \delta P2)^2 + (\delta H1 - \delta H2)^2 \quad (1)$$

where the factor of four on the dispersion term is empirical. Each polymer is characterized by an interaction radius R0, and the relative energy difference RED = Ra/R0 predicts behaviour: RED below unity indicates strong interaction and maximum swelling or dissolution, values near unity indicate borderline behaviour, and values well above unity indicate that the solvent will barely penetrate [66]. Representative parameters are given in Table 3. The framework explains several observations that would otherwise look arbitrary, including why dimethyl sulfoxide, with its very high polar term, is so much more aggressive towards cyanoacrylates than toluene is, and why d-limonene, a low-polarity terpene, is effective against EVA encapsulant and is now used as a greener alternative to aromatic solvents in photovoltaic module recycling [39]. It also provides a rational basis for the deep-eutectic solvent systems now being developed for the same purpose [67].

For surface integrity, the risks of solvent methods are chemical rather than mechanical. Polymer substrates may swell, craze or stress-crack in the same solvent that attacks the adhesive; coatings may lift; and a carbon-rich contamination film is left on the recovered surface almost universally, invisible to profilometry and detectable only by surface-sensitive spectroscopy [16, 33].

4.3.2. Acidic and Alkaline Agents

Sodium hydroxide and potassium hydroxide are used at concentrations of roughly 5–20% to soften polyurethanes and epoxies, typically over 30 minutes to several hours depending on bondline thickness and crosslink density. It should be stated clearly that these are strong bases, fully dissociated in aqueous solution, and describing dilute solutions of them as weak is incorrect: a 5% sodium hydroxide solution has a pH above 14. Their action is chemical scission rather than swelling. Hydroxide attacks ester and amide linkages by nucleophilic acyl substitution, which is why anhydride-cured epoxies and polyurethanes are much more susceptible than amine-cured epoxies, whose network contains no readily hydrolysable linkage; subcritical hydrolysis studies show the same selectivity at elevated temperature [48, 68, 65].

The corrosion consequences deserve more attention than they usually receive. Aluminium is amphoteric and dissolves rapidly in alkali, so strongly alkaline debonding on aluminium adherends etches the substrate, destroys the anodic layer where one is present and leaves a measurably rougher surface. Zinc and tin coatings behave similarly. Acidic agents raise the complementary problem, attacking passive films on stainless steel and titanium, dissolving carbonate stone and, in the presence of chloride, initiating pitting. Alkaline agents also leach network-modifying ions from silicate glass and change its surface chemistry permanently. In every case the recovered surface should be checked for both roughness and composition, not roughness alone [33, 32].

Table 3. Representative Hansen solubility parameters used in the selection of debonding solvents

Liquid or polymer	δD (MPa½)	δP (MPa½)	δH (MPa½)	Relevance to debonding
Acetone	15.5	10.4	7.0	Dissolves cyanoacrylates; swells acrylics
Methyl ethyl ketone	16.0	9.0	5.1	General-purpose adhesive softening
Dimethyl sulfoxide	18.4	16.4	10.2	High polar term; aggressive towards cyanoacrylate and cured acrylic
N-methyl-2-pyrrolidone	18.0	12.3	7.2	Strong epoxy swelling agent; regulatory constraints
Dichloromethane	18.2	6.3	6.1	Rapid swelling of epoxy; substantial health and VOC concerns
Toluene	18.0	1.4	2.0	Low polarity; ineffective on polar networks
Ethanol	15.8	8.8	19.4	High hydrogen bonding; limited penetration of epoxy
d-Limonene	17.2	1.8	4.3	Bio-derived; effective on EVA encapsulant
Water	15.5	16.0	42.3	Non-solvent for most adhesives; carrier for alkaline and enzymatic systems
Poly(methyl methacrylate)	18.6	10.5	7.5	Substrate at risk when acrylics are targeted
Cured DGEBA epoxy (typical)	18–20	9–12	8–11	Swells only; cannot dissolve

Solvent values are the standard tabulated parameters [66]; polymer values are indicative, since they depend on formulation, cure schedule and crosslink density.

4.3.3. Enzymatic and Bio-Inspired Routes

Enzymatic debonding uses proteases, esterizes and lipases to cleave hydrolysable linkages in the adhesive under mild aqueous conditions, near neutral pH and close to ambient temperature. Because the enzyme is selective for particular bonds, the substrate is essentially unaffected, which makes the approach attractive for biomedical components where residual chemical contamination is unacceptable [12, 13]. An enzymatic delamination process has been demonstrated for crystalline-silicon photovoltaic modules, releasing the glass and cells without the solvent load of conventional routes [69]. The limitations are kinetic and economic: reaction times are long, enzyme cost is high, activity is sensitive to temperature and pH, and only adhesives containing hydrolysable linkages are susceptible, which excludes amine-cured epoxy and silicone.

4.4. Electrochemical Debonding

Electrochemical methods remain the least investigated of the five families, which is unfortunate, because on metallic substrates they combine short process times with essentially no mechanical loading. The configuration is shown in Figure 7.

4.4.1. Electrolytic Debonding

In electrolytic debonding the bonded assembly is made one electrode of an electrochemical cell and a potential is applied across the joint in the presence of an electrolyte that has access to the bondline, either through a conductive adhesive, through the joint edges, or through the substrate itself. Faradaic reactions then occur at the buried metal-adhesive interface. Water electrolysis is thermodynamically possible above 1.23 V and proceeds at a useful rate once kinetic overpotentials are exceeded, so hydrogen is evolved at the cathode and oxygen at the anode directly beneath the

adhesive layer [70]. Two effects follow. Gas nucleates in the confined space at the interface and generates local pressure that lifts the adhesive mechanically, and the pH shifts sharply at the electrode surface, becoming strongly alkaline at the cathode, which degrades the interfacial oxide and hydrolyses susceptible linkages in the adhesive. The combination is efficient: separation is often achieved in seconds to a few minutes [70, 38].

Reported operating windows are summarized in Table 4. They should be read as the range encountered across the studies surveyed rather than as recommended settings, since the optimum depends strongly on the adhesive formulation and on the conductivity of the path to the interface.

Table 4. Operating parameters reported for electrolytic debonding, and their effect

Parameter	Range reported in the surveyed literature	Principal effect
Electrolyte	Aqueous NaCl, Na_2SO_4 or $NaNO_3$, typically 0.1–1 M	Sets ionic conductivity and the available anion chemistry; chloride raises pitting risk
Applied voltage	Approximately 5–50 V DC	Must exceed the water decomposition potential plus overpotentials; higher voltage accelerates gas evolution
Current density	Of the order of 1–50 mA/cm^2	Controls the rate of gas generation and therefore the debonding time
Process duration	Tens of seconds to tens of minutes	Scales inversely with current density and with the accessibility of the interface
Polarity	Cathodic or anodic on the workpiece	Cathodic operation evolves hydrogen and raises interfacial pH; anodic operation risks dissolution of the substrate
Temperature	Ambient to about 60 °C	Raises reaction kinetics and diffusion, at the cost of adhesive softening that may be desirable or not

The risks are specific and, in our reading, insufficiently discussed in the debonding literature. Cathodic operation evolves nascent hydrogen at the metal surface, and on high-strength steels, martensitic stainless steels and titanium alloys, atomic hydrogen absorbed into the lattice causes embrittlement, reducing ductility and fracture toughness without leaving any visible mark on the surface. A component recovered by cathodic debonding and returned to service may therefore be degraded in a way that no roughness or spectroscopic measurement will detect, and a post-process bake-out is the standard mitigation. Anodic operation avoids hydrogen but dissolves the substrate. Where dissimilar metals are present in the same electrolyte, the applied field superimposes on the natural galvanic couple and accelerates corrosion of the less noble member. Finally, localized dissolution and gas-evolution pitting increase roughness in patches rather than uniformly, which is why area-averaged Ra can look acceptable while the surface carries discrete pits [70, 33].

4.4.2. Electrochemically Switchable Adhesives

A separate and more elegant strategy designs the adhesive so that its adhesion can be switched off electrically rather than overcome mechanically. Redox-active polymers, ferrocene-containing and viologen-containing formulations, conducting polymer systems and mussel-inspired catechol chemistries all change their interfacial interaction when oxidized or reduced, and reductions in debonding force exceeding 90% under an applied potential have been reported [22, 38, 71]. Because the adhesion is switched rather than destroyed, the recovered surface is often indistinguishable from the pre-bonding condition, which is the best surface integrity outcome available from any method reviewed here. The constraint is architectural rather than chemical: the joint has to be designed from the outset with electrical contacts and an ionically conductive path, so the approach applies to new products designed for disassembly and not to the legacy assemblies that make up most of the practical debonding workload [21, 20].

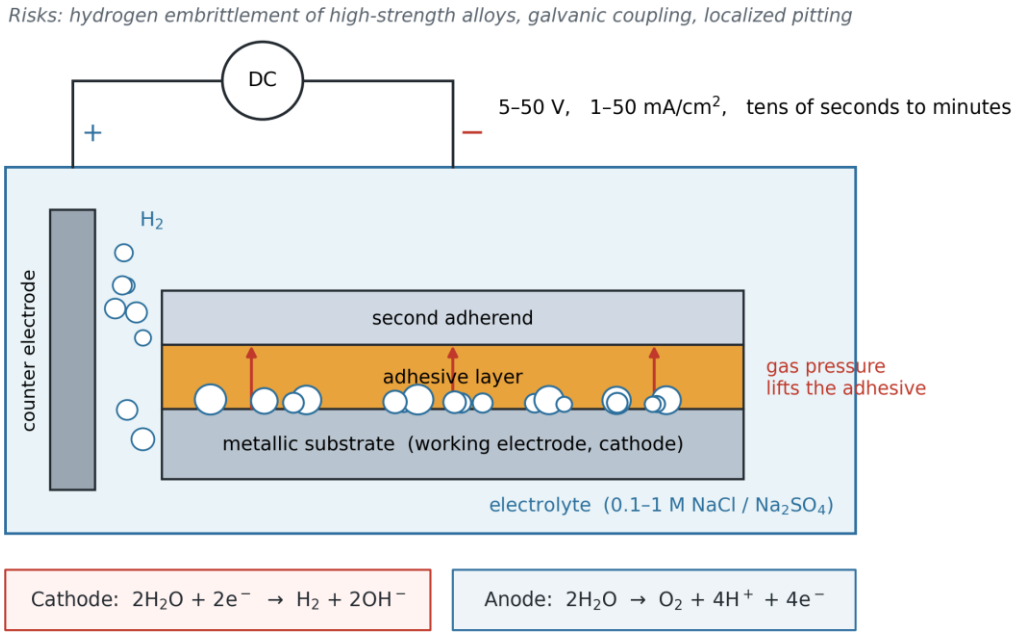

Fig. 7. Electrolytic debonding: the applied potential drives faradaic reactions at the buried interface, hydrogen and oxygen nucleate within the confined bondline, and the resulting local pressure lifts the adhesive while the interfacial pH shift degrades the oxide-adhesive bond

4.5. Hybrid Methods

4.5.1. Laser-Chemical Hybrid Debonding

In this combination a low-fluence laser scan perforates the adhesive layer with an array of micro-channels, and solvent introduced afterwards reaches the interface by diffusion through those channels rather than by the much slower route from the joint edge. Reported reductions in process time relative to solvent immersion alone reach about 70% [19, 36].

The surface integrity outcome depends entirely on the laser fluence, and the apparent contradiction between reports of increased roughness and reports of near-baseline roughness resolves once the two regimes are separated. If the fluence is set high enough for the beam to reach and act on the substrate, the perforations are transferred into the surface and roughness increases measurably. If the fluence is held below the substrate ablation threshold, so that perforation terminates within the adhesive layer, the substrate is not addressed by the beam at all and the recovered roughness stays close to the original, with increments of approximately 0.08 μm reported across metallic, composite and glass substrates [36, 60]. Fluence control, rather than the hybrid concept itself, is therefore the critical process variable, and studies that do not report fluence relative to the substrate threshold are difficult to compare.

4.5.2. Thermal-Mechanical Hybrid Debonding

Moderate heating reduces the adhesive modulus by one to two orders of magnitude as the glass transition is approached, so a mechanical separation that would have damaged the substrate at room temperature can be achieved at much lower force. Reductions in separation force exceeding 60% are reported, with post-debonding roughness within about 15% of the pre-bonding baseline for epoxy removal from carbon-fibre composite substrates [19, 50]. The approach is attractive industrially because it uses equipment that most workshops already have.

4.5.3. Ultrasonic-Chemical Hybrid Debonding

Immersing the assembly in a solvent bath driven at 20–80 kHz couples' cavitation-enhanced mass transport to chemical softening: the acoustic field continually refreshes solvent at the interface and disrupts the diffusion boundary layer, so the rate-limiting step of static immersion is removed.

Reductions in residual surface contamination of up to about 85% relative to static immersion have been reported, with correspondingly high cleaning efficiency on precision optical and medical device surfaces [39, 53]. This combination is, on the evidence surveyed, the most effective route where residue-free recovery matters more than absolute speed.

5. Characterization of the Recovered Surface

No single technique characterizes a debonded surface adequately, and the reason is worth making explicit: the techniques do not look at the same material. A stylus profilometer averages over several micrometers of relief; X-ray photoelectron spectroscopy interrogates the outermost few nanometers; residual stress measured by X-ray diffraction integrates over some tens of micrometers of depth. Two studies reporting contradictory conclusions about the same process may simply be measuring different things. Figure 8 compares the information depth of the principal techniques, and we suggest that any post-debonding assessment should combine at least one topographic, one mechanical and one chemical method chosen from different depth regimes.

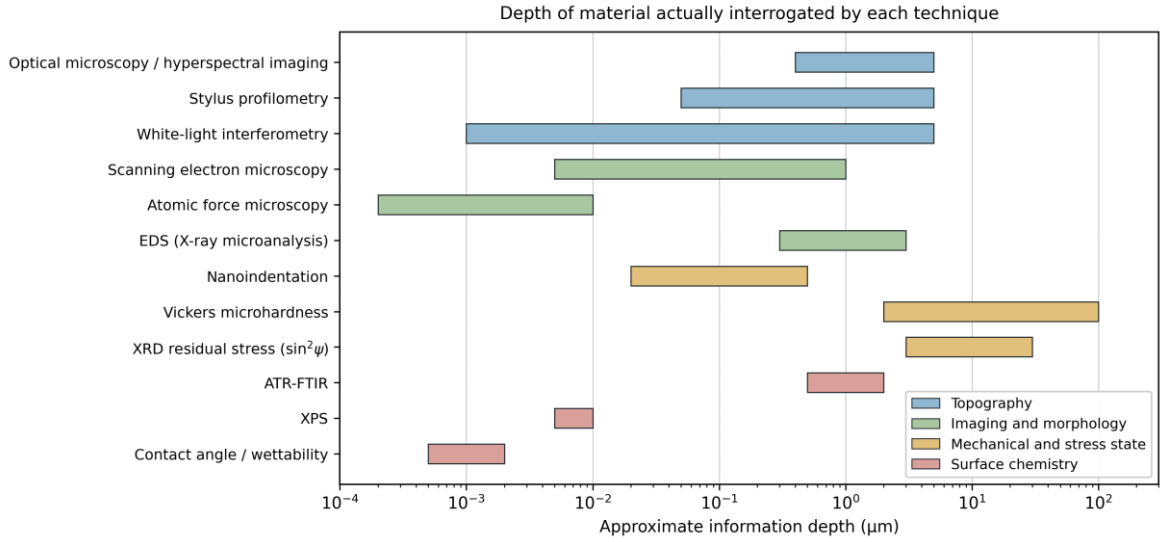

Fig. 8. Information depth of the principal characterization techniques used to assess debonded surfaces, plotted on a logarithmic depth scale. Techniques probing different depths answer different questions and are not interchangeable

5.1. Roughness and Topography

Contact stylus profilometry and non-contact white-light interferometry or confocal microscopy provide the parameters that dominate the debonding literature: Ra, Rq, Rz and the reduced peak height Rpk. Ra is the most reported and the least informative, since it is insensitive to the distinction between a uniformly matt surface and a smooth surface carrying isolated deep scratches; Rz and Rpk, or a full areal analysis to ISO 25178, capture that difference. Across the studies compiled in Section 6, laser and electrochemical routes produced the smallest roughness increments, of the order of 0.05 µm, while mechanical scraping produced the largest, up to about 2.3 µm [19, 52].

5.2. Atomic Force Microscopy

Atomic force microscopy resolves the nanometer-scale features that profilometry cannot see. It is the appropriate technique for detecting nanoscale islands of residual adhesive, shallow scratches below the profilometer detection threshold, and changes in the fine texture of a polished or as-drawn surface. It has been used directly for exactly this purpose in studies of enamel surface roughness after adhesive removal [43]. The trade-off is scan area: a typical AFM field is tens of micrometers square, so the technique characterizes a sample of the surface rather than the surface, and it should be used alongside, not instead of, an area-averaging method.

5.3. Scanning Electron Microscopy And EDS

Scanning electron microscopy visualizes micro-scratches, the distribution of adhesive residue, pitting and coating delamination zones directly, over fields ranging from the whole joint footprint to individual features. Coupled energy-dispersive X-ray spectroscopy adds elemental mapping and identifies carbon-rich contamination layers that a roughness measurement would miss entirely [33]. Its limitations should be kept in view: the interaction volume of EDS extends roughly one micrometer into the material, so it is not a surface technique in the sense that XPS is, and it cannot detect sub-monolayer contamination. Non-conductive substrates require a conductive coating, which is destructive of the surface being assessed.

5.4. Microhardness and Nanoindentation

Vickers microhardness testing under loads of 10–500 gf allows a hardness depth profile to be constructed and reveals subsurface work hardening or thermal softening produced by the debonding operation [27]. Nanoindentation extends the same measurement to penetration depths of tens to hundreds of nanometers and returns modulus as well as hardness, which makes it the only mechanical technique capable of characterizing the outermost layer where a thermally altered or chemically degraded zone would sit.

5.5. Residual Stress

X-ray diffraction using the $\sin^2\psi$ method provides non-destructive near-surface stress measurement and is the standard technique for the purpose. Reported values distinguish the method families clearly: tensile residual stresses of up to approximately 180 MPa have been reported following mechanical scraping, against compressive or near-zero states after laser and electrochemical debonding [28, 27]. The substrate-specific limitation is fundamental rather than practical, and is discussed in Section 5.8.

5.6. Surface Chemistry: XPS and FTIR

X-ray photoelectron spectroscopy quantifies elemental composition and chemical state within the outermost 5–10 nm and detects adhesive contamination at sub-monolayer coverage. It is the reference technique for answering the question that matters most after chemical debonding, namely whether the surface is actually clean [33]. Attenuated total reflectance FTIR complements it by identifying specific polymer residues and solvent degradation products through their vibrational signatures, at sensitivities well below the EDS detection threshold [72]. Where these two techniques have been applied to solvent-debonded surfaces, they have consistently found residual organic films on surfaces that appeared clean by every other measure.

5.7. Optical Inspection and Wettability

High-resolution optical microscopy in brightfield, darkfield and differential interference contrast modes detects micron-scale surface features rapidly and at low cost, and remains the first-line inspection method in production. Hyperspectral imaging extends optical inspection to chemical discrimination, resolving reflectance spectra spatially and identifying contaminant and oxidation zones; it has been demonstrated for quantifying organic contamination on copper surfaces in electronics manufacture, which is close to the debonding verification problem [72]. Contact angle measurement by the sessile drop method is the simplest and most sensitive routine indicator of surface chemical change: organic solvent debonding leaves hydrophobic contamination that has been reported to increase water contact angles by up to 35 degrees on smooth aluminium alloy, whereas ultraviolet laser debonding produces strongly hydrophilic surfaces through photochemical oxidation [33, 26].

5.8. Substrate-Specific Limitations

Technique selection cannot be separated from substrate class, and several of the inconsistencies in the published data appear to arise from this. X-ray diffraction residual stress analysis requires long-range crystalline order, so it applies to metals and to crystalline ceramics but returns nothing for amorphous polymers, silicate glass or the polymer matrix of a composite; residual stress in those materials has to be inferred by other means, such as curvature methods or photoelasticity for

transparent substrates. Energy-dispersive spectroscopy struggles with light-element organic residues on light-element substrates, which is exactly the polymer-on-polymer case. Conductive coating requirements make SEM awkward for glass and polymers. XPS and ATR-FTIR are the only techniques that work across all six substrate classes and detect residue reliably, and we regard them as the minimum chemical requirement for any credible claim of residue-free debonding. Stylus profilometry, finally, damages soft polymer surfaces during the measurement itself, so non-contact methods should be preferred there.

6. Comparative Analysis

Comparing debonding methods across the literature is difficult for a reason that recurs throughout this review: there is no standard test. Substrates, adhesives, bondline thicknesses, baseline roughness and measurement protocols all differ between studies, and absolute values are therefore not strictly commensurable. What is robust is the ordering between method families, which is consistent across independent studies. The comparison below uses six criteria: debonding efficiency, preservation of surface integrity, substrate compatibility, operational cost, environmental and safety burden, and industrial scalability.

6.1. Mechanical Methods

Mechanical routes are the simplest and cheapest and carry the highest risk to the substrate. Scraping raised Ra by roughly 0.3–2.3 μm across the studies surveyed, and also introduced the highest tensile residual stresses of any family. Ultrasonic vibration is the exception within the family and achieved increments as low as about 0.2 μm on smooth metallic and composite substrates, because no tool touches the surface [53, 19]. Controlled peeling sits in between, and its performance is governed by peel angle more than by any other variable [49].

6.2. Thermal Methods

Thermal performance is the most variable of the five families, which reflects how differently energy is delivered within it. Convective heating is inexpensive and scalable but heats the substrate more than the bondline. Laser debonding consistently returns surface roughness within 0.05–0.15 μm of baseline and, in wafer release, below 1 nm Ra, making it the best single-mechanism performer in the review [57, 58, 36]. Induction heating gives rapid cycles but is restricted to conductive substrates or to formulations carrying susceptor particles, with the residue consequences discussed in Section 4.2.3. Cryogenic debonding is the gentlest thermal route in surface terms and the most constrained by assembly geometry [50].

6.3. Chemical Methods

Chemical routes eliminate mechanical damage entirely, which is their principal attraction on brittle and optically finished substrates, but they substitute a contamination problem for a topographic one. Organic residue is detectable by XPS on essentially every solvent-debonded surface reported, even after cleaning [33]. Strongly alkaline and acidic agents add a corrosion penalty that is substrate-specific and, on aluminium, severe. Enzymatic routes have the best substrate compatibility of any method in this review and the worst kinetics and reagent economics [69].

6.4. Electrochemical Methods

Electrochemical debonding is the least investigated family and the one where the gap between demonstrated potential and industrial use is widest. Assemblies built with switchable adhesives recover surfaces that are, within measurement resolution, indistinguishable from the pre-bonding condition [22, 38]. The requirement for integrated electrical contacts confines the approach to designed-for-disassembly products, and the hydrogen embrittlement and galvanic risks set out in Section 4.4.1 restrict electrolytic variants on high-strength alloys.

6.5. Hybrid Methods

Hybrid methods outperform single-mechanism approaches consistently, and the reason is structural rather than incidental: each component addresses a different rate-limiting step. The laser-chemical hybrid recovered Ra within approximately 0.08 μm of baseline across metallic,

composite and glass substrates when the fluence was held below the substrate threshold [36, 60]. The thermal-mechanical hybrid reduced separation force by more than 60% [50], and the ultrasonic-chemical hybrid reduced residual contamination by up to 85% relative to static immersion [39, 53]. The cost is process complexity and a larger parameter space to control.

6.6. Comparative Summary

Table 5 summarizes the qualitative performance of each method against the six criteria, and Table 6 collects the quantitative roughness evidence on which the surface integrity ratings rest. Figure 9 presents the same qualitative comparison graphically.

Table 5. Comparative performance of debonding methods against six evaluation criteria. All criteria are oriented so that a higher rating is more favorable

Debonding method	Debonding efficiency	Surface integrity	Substrate compatibility	Low operational cost	Environmental and safety	Industrial scalability
Controlled peeling	Moderate	Good	Limited	Excellent	Excellent	Moderate
Mechanical scraping	Good	Poor	Good	Excellent	Excellent	Good
Ultrasonic vibration	Good	Good	Good	Moderate	Good	Good
Pneumatic and hydraulic	Moderate	Excellent	Moderate	Moderate	Excellent	Moderate
Convective heating	Good	Moderate	Moderate	Good	Good	Good
Laser debonding	Excellent	Excellent	Excellent	Limited	Good	Moderate
Induction heating	Good	Excellent	Limited	Moderate	Good	Good
Cryogenic debonding	Good	Excellent	Moderate	Moderate	Excellent	Moderate
Solvent chemical	Good	Moderate	Good	Good	Poor	Good
Acidic and alkaline	Good	Limited	Limited	Good	Poor	Moderate
Enzymatic	Moderate	Excellent	Excellent	Poor	Excellent	Limited
Electrolytic	Moderate	Excellent	Limited	Moderate	Good	Limited
Switchable adhesive	Excellent	Excellent	Moderate	Limited	Excellent	Limited
Laser-chemical hybrid	Excellent	Excellent	Excellent	Limited	Moderate	Moderate
Thermal-mechanical hybrid	Good	Good	Good	Good	Good	Good
Ultrasonic-chemical hybrid	Excellent	Excellent	Good	Moderate	Moderate	Good

6.7. Interpretation and Trade-Offs

Three patterns emerge from Tables 5 and 6, and they are more useful than any single ranking.

The first is that surface integrity and cost are inversely related across almost the whole range. The methods that recover the best surfaces, laser, laser-chemical hybrid, switchable adhesives and enzymatic routes, are also the most capital-intensive or the most demanding in reagent cost, while the methods available in every workshop are the ones that damage the substrate most. The break-even point is set by the value of the recovered part. For a precision optics, a thinned wafer or a titanium aerospace fitting, the capital cost of a laser station is recovered on a small number of components; for a bonded automotive sill destined for material recycling, it never is, and a thermal-mechanical route is the rational choice [24].

The second is that no method is simultaneously fast, gentle and broadly applicable. Laser processing is fast and gentle but line-of-sight, so it cannot reach a buried bondline. Chemical routes reach anywhere but are slow and leave residue. Electrochemical routes are fast and gentle but require a conductive path designed in from the start. The apparent superiority of hybrid methods comes precisely from pairing techniques whose constraints do not overlap.

The third is that the environmental ranking has begun to override the technical one. Solvent and strong-acid or strong-base routes score well on cost and compatibility but poorly on environmental burden, and tightening volatile organic compound regulation is progressively removing them from the available options regardless of their technical merit [73]. Methods that looked uncompetitive on cost alone a decade ago, including enzymatic and deep-eutectic-solvent routes, are becoming attractive on this basis [69, 67].

Table 6. Quantitative surface integrity outcomes reported for the principal debonding methods on smooth substrates

Method	Reported roughness change	Residual stress state	Chemical residue	Typical process time
Mechanical scraping	Ra increase of about 0.3–2.3 µm	Tensile, up to approximately 180 MPa	Embedded tool and adhesive debris	Minutes, operator dependent
Controlled peeling	Small increase; strongly peel-angle dependent	Low, localized at the peel front	Adhesive transfer film	Seconds to minutes
Ultrasonic vibration	Ra increase of about 0.2 µm	Low	Reduced when performed in a liquid bath	Seconds to minutes
Convective and conductive heating	Negligible on metals; distortion risk on polymers	Low; thermal gradients possible	Softened adhesive film	Minutes
Laser debonding	Within 0.05–0.15 µm of baseline; below 1 nm Ra in wafer release	Compressive or near zero	Minimal; photo-oxidized surface after UV processing	Seconds
Induction heating	Negligible increase on aluminium alloy	Low	Susceptor particles remain in the residue	Under 60 s
Cryogenic debonding	No measurable change reported	Low	None; no reagents used	Minutes
Solvent chemical	No mechanical change; swelling of polymer substrates possible	None introduced	Carbon-rich film detectable by XPS	30 min to several hours
Alkaline and acidic	Increase through etching, substrate dependent	None introduced	Ionic residue; altered oxide	30 min to several hours
Electrolytic	Small area-averaged increase; localized pitting possible	Low; hydrogen uptake risk	Electrolyte salts requiring rinsing	Seconds to minutes
Switchable adhesive	Indistinguishable from pre-bonding condition	None introduced	Minimal	Seconds
Laser-chemical hybrid	Within about 0.08 µm of baseline below the substrate ablation threshold	Compressive or near zero	Reduced relative to solvent alone	Reduced by up to about 70% versus solvent alone
Thermal-mechanical hybrid	Within about 15% of baseline on CFRP	Low	Softened adhesive film	Separation force reduced by more than 60%
Ultrasonic-chemical hybrid	No mechanical damage reported	None introduced	Contamination reduced by up to about 85% versus static immersion	Minutes

Values are compiled from the sources cited in Sections 4 and 6. Because test conditions differ between studies, the table should be read as an ordering between method families rather than as a set of directly comparable measurements.

6.8. Method Selection Guidance

For high-value substrates with tight surface specifications, such as optical glass, thinned wafers and precision metallic components, laser and laser-chemical hybrid processing are justified despite their capital cost. For high-volume production with moderate surface requirements, ultrasonic-chemical and thermal-mechanical hybrids offer the better cost-benefit balance. For temperature-sensitive assemblies, cryogenic, electrochemical and enzymatic routes avoid the thermal load altogether. For products still at the design stage, designing in a debonding trigger, whether thermal,

electrical or photochemical, converts the problem from one of removal to one of actuation and gives by far the best surface integrity outcome [21, 22, 20].

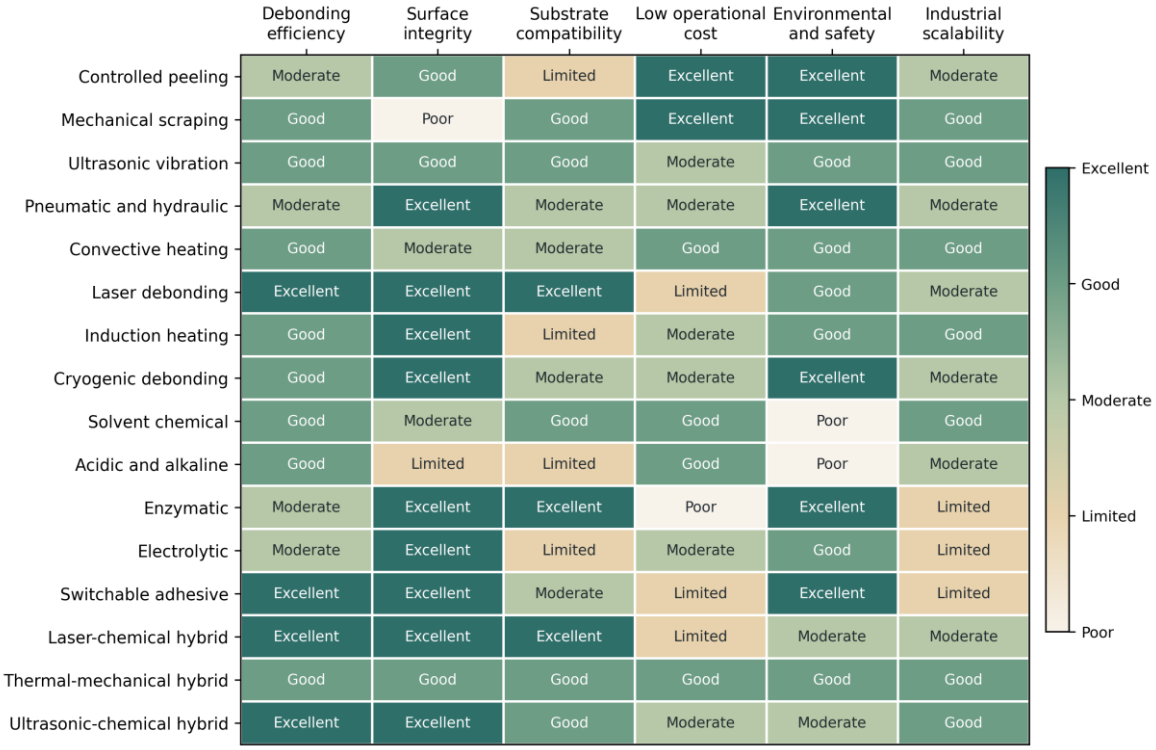

Fig. 9. Comparative performance of debonding methods across the six evaluation criteria of Table 5. Darker cells indicate more favourable performance for that criterion

7. Applications and Industrial Relevance

The requirements placed on a debonding process differ so widely between sectors that a method which is standard practice in one is inadmissible in another. Table 7 summarizes the combinations that recur in industrial practice.

7.1. Aerospace and Defence

Aerospace presents the most demanding combination of requirements in the review. Aluminium alloy, titanium and CFRP substrates must be freed of adhesive completely, without any increase in roughness or microstructural change that would compromise fatigue performance, and usually so that the component can be rebonded [3, 6]. Laser methods are the most promising route for composite repair preparation, since they remove the adhesive without touching the fibre and leave a surface whose chemistry favors rebonding [25, 5]. The recurring difficulty is access: bond lines inside a wing box are not in line of sight.

7.2. Automotive

Windscreen replacement is the highest-volume debonding operation carried out anywhere, and it is instructive because both adherends must survive. The polyurethane bead has to be severed while the electrocoat and topcoat on the painted flange remain intact. Optimized heated-wire cutting confines paint damage to under 2 mm of flange width, against 8–15 mm for cold-knife methods, which is the difference between a repair and a repaint [4, 50]. Multi-material body structures combining steel, aluminium and CFRP are substantially harder, because a single stimulus applied to the whole assembly cannot be optimal for every interface within it [24].

7.3. Electronics and Microelectronics

Semiconductor manufacture applies effectively zero-tolerance contamination standards. Device wafers thinned to 50 µm or less are bonded to transparent carriers and released optically after

processing, with the recovered surface held below 0.3 nm Ra, a level of surface preservation no other method approaches [7, 57], [58, 8]. Thermally releasable polyimide systems and laser-sensitive release layers now compete for the same process step [9, 42].

7.4. Biomedical and Healthcare

Here the criterion shifts from topography to chemistry and to the substrate's own fragility. Medical adhesive-related skin injury is a recognized clinical problem, and silicone-based adhesive removers cause substantially less disruption of the stratum corneum than mechanical peeling does, which matters particularly for neonatal and elderly patients [10, 11]. For implantable and surgical adhesives, freedom from residual chemical contamination is a regulatory requirement rather than a quality target [12, 13].

7.5. Construction and Architecture

Structural silicone removal from glass and aluminium curtain-wall systems is the archetypal case of a smooth, brittle, high-value substrate. Combining chemical softening with plastic scraping tools has been reported to limit Ra increments to about 0.05 µm, against more than 0.8 µm where steel tools are used alone [14, 40]. Laser methods preserve historic substrate surfaces without measurable alteration, which is why they have been adopted in conservation practice [32]. In-service inspection of these joints has its own developed literature based on laser-excited thermography [15, 41].

7.6. Renewable Energy

Photovoltaic module recycling is the fastest-growing application of debonding technology, driven by the volume of modules now reaching end of life. Thermal separation of the EVA encapsulant recovers more than 99% of the glass by mass, while controlled swelling under sonication, particularly with bio-derived limonene, offers a lower-temperature and greener alternative [39, 17], [74, 75]. Deep-eutectic solvents and enzymatic delamination are both under active development for the same purpose [67, 69]. At the other extreme of scale, removal of leading-edge protection film from wind turbine blades exceeding 80 m in length requires robotic implementation simply to achieve consistent results over the length of the blade [76]. Figure 10 illustrates the debonding-on-demand concept in a recycling context.

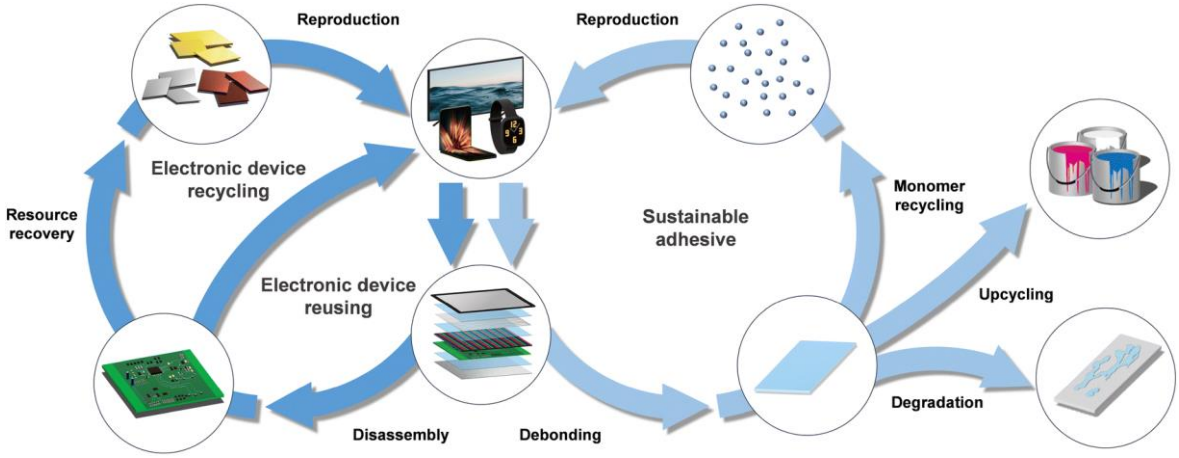

Fig. 10. Debonding-on-demand adhesives applied to disassembly and recycling

7.7. Optics and Precision Instrumentation

Optical instrumentation imposes the tightest specification of all, with Ra below 0.5 nm required and effectively no tolerance for surface damage, since a change in surface figure of a few nanometers is directly visible in an interferometric measurement. Thermal cycling protocols and cryogenic separation have both been shown to release adhesives without measurable modification of surface figure [34, 35, 64].

Table 7. Recommended debonding routes by industrial sector

Sector	Typical substrate	Typical adhesive	Recommended debonding route	Governing constraint
Aerospace and defence	Al and Ti alloys, CFRP	Structural epoxy, film adhesive	Laser; thermal-mechanical hybrid	Fatigue performance and rebondability
Automotive glazing	Painted steel or aluminium flange, glass	Polyurethane	Heated-wire cutting; low-temperature debonding	Survival of the paint system
Automotive body structure	Multi-material steel, Al, CFRP	Toughened epoxy, structural acrylic	Thermal-mechanical; induction with susceptor fillers	Multi-material compatibility and cost
Microelectronics	Thinned Si wafer, glass carrier	Temporary bonding polymer, release layer	Laser release through the carrier	Sub-nanometer roughness and zero contamination
Biomedical devices and skin	Polymer housings, skin	Silicone and acrylic PSA	Silicone-based remover; enzymatic	Chemical contamination and tissue trauma
Construction and glazing	Float glass, anodized aluminium	Structural silicone	Chemical softening with plastic tooling; laser for heritage work	Brittleness and appearance
Photovoltaic recycling	Solar glass, silicon cells	EVA encapsulant	Thermal separation; limonene swelling under sonication; deep-eutectic solvents	Throughput and environmental burden
Wind energy	GFRP blade shell	Leading-edge protection adhesive	Robotic mechanical and thermal-mechanical	Scale and consistency over 80 m
Precision optics	Fused silica, optical glass	Optical epoxy and cement	Cryogenic and controlled thermal cycling	Surface figure at the nanometer level

8. Challenges and Future Directions

8.1. Current Challenges

8.1.1. Absence of Standardized Evaluation

This is, in our assessment, the single most limiting problem in the field. There is no agreed protocol for what should be measured after debonding, on what area, with which technique, or against what baseline. Studies report Ra without specifying the sampling length; roughness without residual stress; residue by EDS where XPS is required. The consequence is that quantitative comparison across studies is unreliable, as Table 6 makes clear, and that genuinely superior methods cannot be distinguished from well-reported ones. An internationally recognized evaluation framework, defining a minimum set of parameters and reporting conventions, would do more for the field than any new removal technique.

8.1.2. Multi-Material Assemblies

As multi-material construction spreads through aerospace, automotive and electronics, the compatibility requirement increasingly prevents the use of the method that would be optimal for any individual interface. A stimulus applied to a whole assembly must be tolerable for its most sensitive component, which means the process is set by the weakest link rather than by the joint

being separated. Spatially selective and adaptive stimuli, of the kind that scanned laser processing and locally addressed induction can in principle provide, are the obvious response [4, 61].

8.1.3. Verification of Complete Removal

Residual contamination detectable only by XPS or secondary ion mass spectrometry persists across every method family reviewed here. Both techniques are laboratory instruments requiring vacuum, and neither can be placed inline in a production environment. There is therefore no practical way to verify, at production rate, that a debonded surface is clean enough to rebond. Optical and hyperspectral approaches are the most plausible route to closing this gap, since they are fast, non-contact and already used for contamination quantification in electronics [72, 33].

8.1.4. Aged and Environmentally Degraded Joints

Almost all published debonding data are obtained on freshly prepared laboratory specimens, whereas almost all industrial debonding is performed on joints that have been in service for years. Environmental ageing changes mechanical properties, chemical composition and interfacial condition, generally in the direction of increased brittleness and reduced predictability, and moisture-degraded joints behave differently again [25]. Process protocols that adapt to the measured condition of the joint, informed by non-destructive assessment before the operation begins, are needed and largely absent [77].

8.1.5. Regulatory Pressure on Chemical Routes

Tightening volatile organic compound regulation is progressively closing off organic solvent-based methods, independently of their technical performance [73]. The replacement candidates, water-based systems, bio-derived terpenes, deep-eutectic solvents and supercritical fluids, are at very different levels of maturity, and the field needs performance data on them measured against the same surface integrity criteria used for the incumbents [39, 67].

8.2. Future Research Directions

8.2.1. Stimuli-Responsive Adhesive Systems

Designing the debonding trigger into the adhesive rather than applying it from outside is the most promising direction in the field, because it converts an aggressive removal problem into a controlled actuation problem. Photocleavable molecular units, thermally reversible Diels-Alder networks, vitrimer chemistries with exchangeable bonds, responsive microcapsules and magnetically addressable formulations have all been demonstrated [21, 78], [79, 80], [81, 51]. The open questions are no longer whether the chemistry works but whether these systems retain structural performance over a full-service life, and whether the trigger can be guaranteed not to fire accidentally in service, which is the concern that has kept them out of primary structure so far [82, 83].

8.2.2. Machine Learning in Process Optimization

Two applications are developing in parallel. Convolutional networks trained on electron micrographs have been used to classify post-debonding surface condition automatically, with reported accuracies around 94% for wafer surfaces, which points towards inline machine vision assessment. Separately, reinforcement learning and Bayesian optimization have been applied to the selection of laser and plasma process parameters, converging on effective settings with far fewer experiments than a conventional design of experiments requires [26, 84]. The limiting factor in both cases is the availability of labelled datasets, which is itself a consequence of the standardization gap discussed above.

8.2.3. Nanotechnology-Enhanced Routes

Carbon nanotube and graphene-reinforced formulations create percolating conductive pathways through an otherwise insulating adhesive, which extends electrochemical and resistive-heating debonding to non-conductive substrates that could not otherwise be addressed [62, 63]. In a second approach, nanoparticle carriers deliver debonding agents directly to the adhesive-substrate interface, so that the effective local concentration is high while the bulk solvent inventory, and

therefore the environmental burden, stays low. Both raise the residue question addressed in Section 4.2.3 and should be evaluated with it in view.

8.2.4. Robotics and Automation

Large-area debonding in aerospace, automotive and renewable energy applications is currently limited less by the physics of removal than by the variability that manual operation introduces over large areas. Robotic implementation with force-torque feedback and inline process monitoring addresses this directly by holding the process parameters constant regardless of position on the component, and it is a prerequisite for any operation on the scale of a wind turbine blade or a fuselage panel [76, 24].

8.2.5. Sustainable and Bio-Inspired Approaches

Biological adhesion offers working models of reversible attachment that engineered systems have not yet matched. Marine organisms release catechol-based adhesion in response to environmental cues, and the dry adhesive systems inspired by gecko setae attach and detach thousands of times without residue [37, 82, 71]. Translating these mechanisms into structural adhesives that survive an industrial service environment is the outstanding challenge. In the nearer term, integrated platforms combining laser debonding, atmospheric plasma reactivation and inline spectroscopic verification appear to us the most realistic route to a closed-loop process in which a component is separated, verified and rebonded without leaving the production line [26, 72].

9. Conclusion

This review examined adhesive debonding from smooth substrates with the condition of the recovered surface, rather than the speed of separation, as the criterion of success. Taking that view changes the ranking of the available methods considerably.

Substrate class and adhesive chemistry jointly determine what is admissible. Smooth substrates are a distinct problem because adhesion is carried by short-range interactions distributed uniformly across a nearly planar interface, which removes the natural crack initiation sites that debonding processes exploit, while simultaneously reducing the tolerance for damage to a level at which a single scratch is a failure. Adhesive chemistry sets the available trigger: covalently crosslinked thermosets can be swollen but not dissolved, thermoplastic systems remain reversible, and silicones resist complete removal in every method surveyed.

Among the method families, mechanical routes are simple and cheap but degrade the surface most severely, with ultrasonic vibration the clear exception within the family. Thermal methods vary widely, and laser debonding is the best single-mechanism performer, returning roughness within 0.05–0.15 μm of baseline and below 1 nm in wafer release. Chemical methods eliminate mechanical damage but substitute a contamination problem and, in strongly alkaline or acidic form, a corrosion problem. Electrochemical methods, particularly switchable adhesive systems, produce the best surfaces of all but require the joint to be designed for them, and electrolytic variants carry hydrogen embrittlement and galvanic risks that are not always acknowledged. Hybrid methods consistently outperform single-mechanism approaches because they pair techniques whose limitations do not overlap, with laser-chemical and ultrasonic-chemical combinations the strongest performers.

Assessment of the recovered surface requires several complementary techniques chosen from different depth regimes, since no single parameter captures the range of modification that debonding can produce, and since techniques that probe different depths answer different questions. We would argue that a credible claim of surface-preserving debonding requires at minimum an aerial topographic measurement, a subsurface mechanical or residual stress measurement, and a surface-sensitive chemical measurement.

Industrial demand across aerospace, automotive, electronics, biomedical, construction, renewable energy and precision optics continues to grow, and the technical literature is expanding with it. What is not expanding at the same rate is the methodological basis for comparing results between studies. Until a standardized post-debonding evaluation protocol exists, the field will continue to accumulate empirical, application-specific procedures that cannot be transferred between

substrates or sectors. Establishing that protocol, and coupling it to the developing work on responsive adhesives, inline verification and greener chemistries, is in our view the most productive direction for the next several years of research.

References

[1] Da Silva LFM, Oechsner A. Adhesive bonding technology review. Discov Mech Eng. 2023;2(1):14. https://doi.org/10.1007/s44241-023-00014-5

[2] Campilho RDSG, Madani K, Prakash C. Advanced characterization of adhesive joints and adhesives. Materials (Basel). 2022;15(20):7347. https://doi.org/10.3390/ma15207347

[3] Orsatelli JB, Paroissien E, Lachaud F, Schwartz S. Bonded flush repairs for aerospace composite structures: a review on modelling strategies and application to repairs optimization, reliability and durability. Compos Struct. 2023;304(Pt 2):116338. https://doi.org/10.1016/j.compstruct.2022.116338

[4] Jang YY, Ha JC, Lee D, Lee Y, Nam SY, Yang SB, Kwon DJ. Dissimilar material bonding technology for lightweight future mobility: a review. Polym Test. 2023;129:108281. https://doi.org/10.1016/j.polymertesting.2023.108281

[5] Singh G, Prakash S, Mendiratta M. Adhesive bonding of laser pretreated AA5754 and CFRP surfaces under different processing environments. Int J Adhes Adhes. 2026;104288. https://doi.org/10.1016/j.ijadhadh.2026.104288

[6] Adeleke OA, Wang J, Chiu WK. Injection repair for advanced aerospace composite materials. J Polym Eng. 2025. https://doi.org/10.1177/09673911251333463

[7] Mo Z, Wang F, Li J, Liu Q, Zhang G, Li W, Yang C, Sun R. Temporary bonding and debonding in advanced packaging: recent progress and applications. Electronics. 2023;12(7):1666. https://doi.org/10.3390/electronics12071666

[8] Enomoto T, Miyazawa E, Akasu Y, Sobue S, Nakamura Y, Kawamori T. Novel temporary bonding/debonding system enabling advanced packaging process. J Photopolym Sci Technol. 2022;35(2):153-159. https://doi.org/10.2494/photopolymer.35.153

[9] Huang D, Liu J, Li J, Wang F, Li K, Liu Q, Sun R. Controlled thermal imidization of thermoplastic polyimide for temporary bonding and debonding in advanced packages. ACS Appl Polym Mater. 2022;4(11):8508-8519. https://doi.org/10.1021/acsapm.2c01415

[10] de Faria MF, Ferreira MBG, Dos Santos Felix MM, Bessa RMV, Barbosa MH. Prevention of medical adhesive-related skin injury during patient care: a scoping review. Int J Nurs Stud Adv. 2022;4:100078. https://doi.org/10.1016/j.ijnsa.2022.100078

[11] Pires-Junior JF, Chianca TCM, Borges EL, Azevedo C, Simino GPR. Medical adhesive-related skin injury in cancer patients: a prospective cohort study. Rev Lat Am Enfermagem. 2021;29:e3500. https://doi.org/10.1590/1518-8345.5227.3500

[12] Li X, Ding J, Xie D, He S, Guo J. Recent progress in polymer-based biomaterials as adhesives. Front Bioeng Biotechnol. 2023;11:1305531. https://doi.org/10.3389/fbioe.2023.1305531

[13] Boursier M, Bayon Y, Negrell C, Pinaud J, Caillol S. Biocompatible glues: recent progress and emerging frontiers in surgical adhesion. Polymers (Basel). 2025;17(13):1749. https://doi.org/10.3390/polym17131749

[14] Wallau W, Recknagel C, Smales GJ. Structural silicone sealants after exposure to laboratory test for durability assessment. J Appl Polym Sci. 2021;138(35):50881. https://doi.org/10.1002/app.50881

[15] Lin J, Hong X, Ren Z. Laser in-depth heating thermal wave detection of adhesive debonding in glass curtain walls: numerical simulation and experiment. Measurement. 2021;177:109268. https://doi.org/10.1016/j.measurement.2021.109268

[16] Novoa FD, Miller DC, Dauskardt RH. Environmental mechanisms of debonding in photovoltaic backsheets. Sol Energy Mater Sol Cells. 2014;120:87-93. https://doi.org/10.1016/j.solmat.2013.08.020

[17] Deng R, Zhuo Y, Shen Y. Recent progress in silicon photovoltaic module recycling processes. Resour Conserv Recycl. 2022;187:106612. https://doi.org/10.1016/j.resconrec.2022.106612

[18] Mulcahy KR, Kilpatrick AFR, Harper GDJ, Walton A, Abbott AP. Debondable adhesives and their use in recycling. Green Chem. 2022;24(1):36-61. https://doi.org/10.1039/D1GC03306A

[19] Srinivasan DV, Idapalapati S. Review of debonding techniques in adhesively bonded composite structures for sustainability. Sustain Mater Technol. 2021;30:e00345. https://doi.org/10.1016/j.susmat.2021.e00345

[20] Kim D, Park Y, Kwon MS. Debonding-on-demand adhesives for recycling and reusing of electronic devices. Mater Horiz. 2025;12(14):4934-4939. https://doi.org/10.1039/D5MH00468C

[21] Blelloch ND, Yarbrough HJ, Mirica KA. Stimuli-responsive temporary adhesives: enabling debonding on demand through strategic molecular design. Chem Sci. 2021;12(46):15183-15205. https://doi.org/10.1039/D1SC03426J

[22] Liu Z, Yan F. Switchable adhesion: on-demand bonding and debonding. Adv Sci (Weinh). 2022;9(12):2200264. https://doi.org/10.1002/advs.202200264
[23] Ghahremani A, Adams SD, Norton M, Khoo SY, Kouzani AZ. Delamination techniques of waste solar panels: a review. Clean Technol. 2024;6(1):280-298. https://doi.org/10.3390/cleantechnol6010014
[24] Jordan A, Hermelingmeier L, Gilich J, Meschut G, De Santis M, Schlueter A. Comparison of the economic efficiency and sustainability of two debonding processes for structurally bonded sills. J Adv Joining Process. 2025;100332. https://doi.org/10.1016/j.jajp.2025.100332
[25] Houjou K, Terasaki N, Horiuchi S, Yase K, Shimamoto K, Akiyama H. Effect of laser treatment on strength of moisture-degraded epoxy adhesive joints and microscopic observation of treated surface. J Adhes. 2025;101(2):379-395. https://doi.org/10.1080/00218464.2024.2304567
[26] Jordens J, Van Doninck B, Satrio NR, Hernandez AM, Couckuyt I, Van Nieuwenhuyse I, Witters M. Optimization of plasma-assisted surface treatment for adhesive bonding via artificial intelligence. In: 2nd International Conference on Industrial Applications of Adhesives 2022. Cham: Springer; 2022. p. 47-64. https://doi.org/10.1007/978-3-031-11150-1_4
[27] Oender S, Saklakoglu N, Sever A. Selective laser melting of Ti6Al4V alloy: effect of post-processing on fatigue life, residual stress, microstructure, microhardness and surface roughness. Mater Charact. 2023;196:112571. https://doi.org/10.1016/j.matchar.2022.112571
[28] Gao Y, Yang W, Huang Z, Lu Z. Effects of residual stress and surface roughness on the fatigue life of nickel aluminium bronze alloy under laser shock peening. Eng Fract Mech. 2021;244:107524. https://doi.org/10.1016/j.engfracmech.2021.107524
[29] Strauss L, Pang GA, Loewisch G. Fatigue life prediction of additively manufactured AlSi10Mg based on surface roughness and residual stress. Fatigue Fract Eng Mater Struct. 2024;47(12):4465-4477. https://doi.org/10.1111/ffe.14441
[30] Wan H, Min J, Lin J, Carlson BE, Maddela S, Sun C. Effect of laser spot overlap ratio on surface characteristics and adhesive bonding strength of an Al alloy processed by nanosecond pulsed laser. J Manuf Process. 2021;62:555-565. https://doi.org/10.1016/j.jmapro.2020.12.050
[31] Zou X, Liu L, Chen T, Wu L, Chen K, Kong L, Wang M. Laser surface treatment to enhance the adhesive bonding between steel and CFRP: effect of laser spot overlapping and pulse fluence. Opt Laser Technol. 2023;159:109002. https://doi.org/10.1016/j.optlastec.2022.108504
[32] Bertasa M, Korenberg C. Successes and challenges in laser cleaning metal artefacts: a review. J Cult Herit. 2022;53:100-117. https://doi.org/10.1016/j.culher.2021.10.010
[33] Geurts KJ, Creemers F, Campestrini P, Van de Weyenberg I, Noeske M, Ihde J, Brune K. Extended non-destructive testing for inline quality control of cleaning and pre-treatment processes in adhesive bonding of polymer blends. SN Appl Sci. 2023;5(1):23. https://doi.org/10.1007/s42452-022-05243-1
[34] Beutel F, Grottke T, Wolff MA, Schuck C, Pernice WHP. Measuring the refractive index of optical adhesives at cryogenic temperatures. Opt Express. 2022;30(17):30066-30074. https://doi.org/10.1364/OE.462163
[35] Lin B, Witt D, Young JF, Chrostowski L. Cryogenic optical packaging using photonic wire bonds. APL Photonics. 2023;8(12):126109. https://doi.org/10.1063/5.0170974
[36] Zhu G, Xu Z, Jin Y, Chen X, Yang L, Xu J, Shan D, Chen Y, Guo B. Mechanism and application of laser cleaning: a review. Opt Lasers Eng. 2022;157:107130. https://doi.org/10.1016/j.optlaseng.2022.107130
[37] Fan H, Gong JP. Bioinspired underwater adhesives. Adv Mater. 2021;33(44):e2102983. https://doi.org/10.1002/adma.202102983
[38] Neubert TJ, Walter K, Schroeter C, Guglielmotti V, Hinrichs K, Reinicke S, Boerner HG. Redox-triggered debonding of mussel-inspired pressure sensitive adhesives: improving efficiency through functional design. Angew Chem Int Ed. 2024;63(44):e202408441. https://doi.org/10.1002/anie.202408441
[39] Min R, Deng W, Wang Z, Qi T, Zhang Z, Xiao W, Qian G, Wang D. Effective decapsulation method for photovoltaic modules: limonene-induced EVA controlled swelling under sonication and debonding mechanism analysis. J Clean Prod. 2024;450:141917. https://doi.org/10.1016/j.jclepro.2024.141917
[40] Karimi S, Liu Y, Kanellopoulos A, Datsiou KC. Thermally activated debonding-on-demand of structural silicone for glass-aluminium joints. Glass Struct Eng. 2026;11(2):11. https://doi.org/10.1007/s40940-026-00330-w
[41] Lin J, Hong X, Ren Z, Chen J. Scanning laser in-depth heating infrared thermography for deep debonding of glass curtain walls structural adhesive. Measurement. 2022;192:110902. https://doi.org/10.1016/j.measurement.2022.110902
[42] Anwar TB, Bardeen CJ. Nanosecond laser debonding using an ultrathin absorber layer in a transparent composite: making a light-powered exploding bolt. Adv Funct Mater. 2024;34(51):2410080. https://doi.org/10.1002/adfm.202410080
[43] Doddavarapu S, Brahmani K, Singaraju GS, Priyanka JSY, Reddy GV, Mandava P, et al. A comparative evaluation of enamel surface roughness of two different bonding adhesives after debonding with atomic force microscopy. Cureus. 2022;14(11):e31661. https://doi.org/10.7759/cureus.31661

[44] Aldosari SM, AlOtaibi BM, Alblalaihid KS, Aldoihi SA, AlOgab KA, Alsaleh SS, Alshammari BA. Mechanical recycling of carbon fiber-reinforced polymer in a circular economy. Polymers (Basel). 2024;16(10):1363. https://doi.org/10.3390/polym16101363
[45] Yuan M, Li Z, Teng Z. Progress and prospects of recycling technology for carbon fiber reinforced polymer. Front Mater. 2024;11:1484544. https://doi.org/10.3389/fmats.2024.1484544
[46] Kanidi M, Loura N, Frengkou A, Milickovic TK, Trompeta AF, Charitidis C. Inductive thermal effect on thermoplastic nanocomposites with magnetic nanoparticles for induced-healing, bonding and debonding on-demand applications. J Compos Sci. 2023;7(2):74. https://doi.org/10.3390/jcs7020074
[47] Borah N, Karak N. Tannic acid based bio-based epoxy thermosets: evaluation of thermal, mechanical, and biodegradable behaviors. J Appl Polym Sci. 2022;139(11):51792. https://doi.org/10.1002/app.51792
[48] Backens S, Wieland AK, Schmidt S, Fluegge W, Friederici L, Rueger CR. Analysis of the decomposition of an anhydride-cured epoxy resin by subcritical hydrolysis. Sci Rep. 2025;15(1). https://doi.org/10.1038/s41598-025-13375-8
[49] Yamada M, Takahashi K, Fujimura N, Nakamura T. Generalized characteristics of peel tests. Eng Fract Mech. 2022;271:108653. https://doi.org/10.1016/j.engfracmech.2022.108653
[50] Bartley A, Chudalla N, Meschut G, Wibbeke TM. Low temperature debonding of toughened structural adhesive joints: a new approach to repairs in the automotive industry. Int J Adhes Adhes. 2023;127:103486. https://doi.org/10.1016/j.ijadhadh.2023.103486
[51] Renken R, Hochheim T, Schaefer S, Hartwig A. Azodicarbonamide-derived crosslinkers for debonding on demand polysiloxane adhesives. React Funct Polym. 2026;227:106862. https://doi.org/10.1016/j.reactfunctpolym.2026.106862
[52] Thys DG, Martins FRP, Cardinal L, Ribeiro GLU. In vitro enamel surface roughness analysis of 4 methods for removal of remaining orthodontic adhesive after bracket debonding. Angle Orthod. 2023;93(2):213-221. https://doi.org/10.2319/031722-227.1
[53] Zhou Z, Chen C. Research advances in the ultrasonic-assisting adhesive bonding. J Manuf Process. 2024;110:134-160. https://doi.org/10.1016/j.jmapro.2023.12.050
[54] Cao Y, Wang H, Zhang Q, Huang K, Chen Y, Wang J, Yan F, Liu H. Study on interfacial interlocking effect of ultrasonic vibration-assisted adhesive bonding. Polymers (Basel). 2022;14(13):2622. https://doi.org/10.3390/polym14132622
[55] Wang H, Tong X, Chen Y, Hua L, Wu M, Ji W. Study on ultrasonic vibration-assisted adhesive bonding of CFRP laminates with laser ablation-treated surfaces. Compos Struct. 2021;268:113983. https://doi.org/10.1016/j.compstruct.2021.113983
[56] Hakkaku T, Mori N, Hayashi T. Ultrasonic layer resonance assisted adhesive bonding for metal plates. Sci Rep. 2025;15(1):33. https://doi.org/10.1038/s41598-025-19688-y
[57] Wang S, Yu Y, Li S, Feng Y, Li J, Yang C, Li W. Laser debonding application in ultra-thin device processing. Appl Opt. 2023;62(23):6140-6146. https://doi.org/10.1364/AO.490195
[58] Zhang J, Hu Y, Wang F, Liu Q, Niu F, Li J, Huang M, Zhang G, Sun R. Precise modulation of the debonding behaviours of ultra-thin wafers by laser-induced hot stamping effect and thermoelastic stress wave for advanced packaging of chips. Int J Extrem Manuf. 2025;7(1):015005. https://doi.org/10.1088/2631-7990/ad8a26
[59] Ma C, Wang F, Liu H, Liu Q, Dai W, Huang M, Sun R. Controlled interfacial debonding based on laser induced deformation-impact coupling effect for advanced packaging. Appl Surf Sci. 2025;165350. https://doi.org/10.1016/j.apsusc.2025.165350
[60] Bi S, Lei Z, Feng J. Comparison and improvement of millisecond pulsed laser and nanosecond pulsed laser for cleaning to remove paint coating from aluminum alloy surface. J Mater Eng Perform. 2024;33(12):5765-5775. https://doi.org/10.1007/s11665-023-08344-z
[61] Gkartzou E, Zafeiris K, Tsirogiannis C, Pedreira A, Rodriguez A, Romero-Rodriguez P, Gakis GP, Kosanovic-Milickovic T, Kyritsis A, Charitidis CA. Induction heating of laminated composite structures with magnetically responsive nanocomposite interlayers for debonding-on-demand applications. Polymers (Basel). 2024;16(19):2760. https://doi.org/10.3390/polym16192760
[62] Lee JS, Kim M, Lee MW. Debonding-on-demand adhesive film using internal Joule heating effect of the steel-aramid braided reinforcement. Compos Struct. 2022;286:115290. https://doi.org/10.1016/j.compstruct.2022.115290
[63] Kachouri O, Bardon J, Ruch D, Laachachi A. Controlling debond on demand performance in adhesive systems using structurally tuned expandable graphite fillers. J Adv Joining Process. 2025;11:100309. https://doi.org/10.1016/j.jajp.2025.100309
[64] Wasserman WW, Harrison RA, Harris GI, Sawadsky A, Sfendla YL, Bowen WP, Baker CG. Cryogenic and hermetically sealed packaging of photonic chips for optomechanics. Opt Express. 2022;30(17):30822-30839. https://doi.org/10.1364/OE.463752

[65] Zhang X, Ma C, Liu P, Huang D, Li P. Recycling of ammonia-cured epoxy resin by oxidative degradation of nitric acid assisted by swelling agent. Eur Polym J. 2023;186:111823. https://doi.org/10.1016/j.eurpolymj.2023.111823
[66] Hansen CM. Hansen solubility parameters: a user's handbook. 2nd ed. Boca Raton (FL): CRC Press; 2007
[67] Yu Y, Shi J, Bai X, Zhang Z, Xi F, Li S, Deng R. Green recycling of end-of-life photovoltaic modules via deep-eutectic solvents - Part B. Chem Eng J. 2025;512:162345. https://doi.org/10.1016/j.cej.2025.162345
[68] Fan T, Zhang H, Gu X, Li X, Guo Y, Ke F, Chen Y, Wang H. Progress in selective depolymerization of epoxy resin for sustainable recycling of carbon fiber reinforced epoxy resin composites. Polym Degrad Stab. 2025;242:111720. https://doi.org/10.1016/j.polymdegradstab.2025.111720
[69] Karagoez SC, Guendogdu TK, Sarialtin H, Celiktas MS. A novel enzymatic delamination method for sustainable recycling of crystal silicon photovoltaic (c-Si PV) modules. Sep Purif Technol. 2025;361:131373. https://doi.org/10.1016/j.seppur.2024.131373
[70] Barnewitz PM, Holtmannspoetter J, Arikan E, Lion A. Electrical induced debonding on demand of adhesive joints for the automotive industry. In: Lecture Notes on Advanced Structured Materials. Cham: Springer; 2025. p. 301-317. https://doi.org/10.1007/978-3-031-77403-4_18
[71] Ge Z, Ren H, Zhang R, Luo C. Designing protein-tannin nanohesives for rapid, universal, and robust wet-adhesion with on-demand debonding. Eur Polym J. 2024;209:112902. https://doi.org/10.1016/j.eurpolymj.2024.112902
[72] Englert T, Gruber F, Stiedl J, Green S, Jacob T, Rebner K, Graehlert W. Use of hyperspectral imaging for the quantification of organic contaminants on copper surfaces for electronic applications. Sensors (Basel). 2021;21(16):5595. https://doi.org/10.3390/s21165595
[73] Guo Y, Zhu L, Zhang L, Tang X, Li X, Ge Y, et al. Temporal variation and industry-specific differences of the use of volatile organic compounds from 2018 to 2023 and their health risks in a typical industrially concentrated area in South China. Toxics. 2024;12(9):634. https://doi.org/10.3390/toxics12090634
[74] Ndalloka ZN, Nair HV, Alpert S, Schmid C. Solar photovoltaic recycling strategies. Sol Energy. 2024;270:112379. https://doi.org/10.1016/j.solener.2024.112379
[75] Chen PH, Chen WS, Lee CH, Wu JY. Comprehensive review of crystalline silicon solar panel recycling: from historical context to advanced techniques. Sustainability. 2024;16(1):60. https://doi.org/10.3390/su16010060
[76] Mishnaevsky L. Root causes and mechanisms of failure of wind turbine blades: overview. Materials (Basel). 2022;15(9):2959. https://doi.org/10.3390/ma15092959
[77] Jasiuniene E, Yilmaz B, Smagulova D, Bhat GA, Cicenas V, Zukauskas E, Mazeika L. Non-destructive evaluation of the quality of adhesive joints using ultrasound, X-ray, and feature-based data fusion. Appl Sci (Basel). 2022;12(24):12930. https://doi.org/10.3390/app122412930
[78] Stamp CH, Stumpp J, Calvino C. Adhesives with debonding-on-demand capability: leveraging responsive microcapsules for mechanically-induced debonding. Adv Mater. 2025;37(13):2414308. https://doi.org/10.1002/adma.202414308
[79] Knight SJ, McCoy JD, Chowdhury S, Lee Y. Debonding-on-demand reversible adhesives via heat or light with competitive adhesion strength to conventional epoxy adhesives. Polym Test. 2025;146:108776. https://doi.org/10.1016/j.polymertesting.2025.108776
[80] Inada M, Horii T, Fujie T, Nakanishi T, Asahi T. Debonding-on-demand adhesives based on photo-reversible cycloaddition reactions. Mater Adv. 2023;4(5):1289-1296. https://doi.org/10.1039/D2MA01048H
[81] Nartam S, Budhe S, Paul J, de Barros S. Strength, repairability, and debonding of vitrimer structural adhesive joints. Academia Mater Sci. 2026;3(2):8358. https://doi.org/10.20935/acadmatsci8358
[82] Skandalis A, Ayer MA, Weder C. Bioinspired adhesives with debonding-on-demand capability. ACS Macro Lett. 2025;14(4):420-427. https://doi.org/10.1021/acsmacrolett.5c00035
[83] Hohl DK, Weder C. (De)bonding on demand with optically switchable adhesives. Adv Opt Mater. 2019;7(16):1900230. https://doi.org/10.1002/adom.201900230
[84] Steege T, Bernard G, Darm P, Kunze T, Lasagni AF. Prediction of surface roughness in functional laser surface texturing utilizing machine learning. Photonics. 2023;10(4):361. https://doi.org/10.3390/photonics10040361